SPECIAL PROJECT PROGRESS REPORT

Progress Reports should be 2 to 10 pages in length, depending on importance of the project. All the following mandatory information needs to be provided.

Reporting year	January to June 2013
Project Title:	High Resolution Regional climate projections at 2 deg C global warming thresholds
Computer Project Account:	spsejone
Principal Investigator(s):	Colin Jones[1], Gunilla Svensson[2] David Lindstedt[1], Petter Lind[1], Patrick Samuelsson[1]
Affiliation:	[1]Swedish Meteorological and Hydrological Institute (SMHI), [2]University of Stockholm
Name of ECMWF scientist(s) collaborating to the project (if applicable)	……………………………………………………….…… ……………………………………………………….……
Start date of the project:	2012-12-31
Expected end date:	2015-12-29

Computer resources allocated/used for the current year and the previous one
(if applicable)
Please answer for all project resources

		Previous year		Current year	
		Allocated	Used	Allocated	Used
High Performance Computing Facility	(units)			12 million	5.4 million
Data storage capacity	(Gbytes)			40 000	92 000

Summary of project objectives
(10 lines max)

The primary aim is to use a new Regional Climate Model (RCM), based on the HARMONIE NWP model, to downscale an ensemble of high-resolution (T511), 30-year global climate timeslices made with EC-Earth as part of the EU FP7 project IMPACT2C. These timeslices use bias-corrected SSTs and Sea Ice (SIC) derived from CMIP5 coupled simulations of the same model, representative of the recent past and two 30 year periods centred on 2°C global warming compared to pre-industrial conditions in respectively the RCP4.5 and RCP8.5 CMIP5 projections. Output from EC-Earth is used to force HARMONIE on a pan-European (Euro-CORDEX) domain, employing a resolution of ~6.25km, to develop a set of 2°C European climate scenarios. The 6.25km HARMONIE simulations will also be used to force smaller HARMONIE domains over sub-regions of Europe run at convection-resolving resolutions (~2km). A key aim is to develop a climate modelling capacity at 'grey-zone' resolutions ~ 3-8km and to investigate convection-resolving climate simulations.

Summary of problems encountered (if any)
(20 lines max)

A number of technical limitations in HARMONIE for application to climate timescales are presently being addressed, these include; (i) treatment of time-varying greenhouse gas concentrations, (ii) representation of regional seas, sea-ice and lakes and (iii) a no-flux lower boundary condition in the HARMONIE soil scheme. All of these limitations do not prevent initial test runs for present climate conditions and are now close to being solved prior to the EC-Earth driven climate projections.

One major technical limitation early in the project was the amount of output needing to be saved and transferred from ECMWF to our local compute system in Sweden. This resulted in intensive use of the ECFS system early in the project. Data is now being transferred to an alternative system. Nevertheless, disk space and the volume of data needed both as boundary conditions for HARMONIE and produced as output by HARMONIE in climate mode remains a serious challenge.

Summary of results of the current year *(from July of previous year to June of current year) This section should comprise 1 to 8 pages and can be replaced by a short summary plus an existing scientific report on the project*

The first months of the project have concentrated on solving a number of technical challenges for running HARMONIE in climate mode at ECMWF and, in particular, assessing the performance of the model at a number of resolutions, using different physical parameterization options, when forced by ERA-interim boundary conditions.

The first 6 months of the allocation builds on work already performed with HARMONIE using the Swedish national allocation at ECMWF. Our initial efforts have concentrated on evaluating the overall performance of HARMONIE for present climate conditions, using the Euro-CORDEX domain. To this end HARMONIE has been run at two resolutions (12.5km and 6.25km) over the Euro-CORDEX domain, driven by ERA-interim lateral and surface boundary conditions, for the period 1997-2008 inclusive. The coarser resolution version allows us to compare HARMONIE performance to our present RCM (RCA4) and to other European RCMs run in Euro-CORDEX at an equivalent resolution forced by ERA-interim. The two HARMONIE resolutions allow us to assess benefits accruing from the increased resolution in a common model. Results from these simulations are close to being submitted as a first article (submission is aimed for September 2013) and a *work-in-progress* version of this manuscript is attached to this report.

HARMONIE contains a number of physics packages, specifically developed for different resolution ranges. In this project we concentrate on the ALARO physics, nominally developed for grey-zone resolutions (~3-10km) and the AROME physics, applicable to convection-resolving resolutions (~1-3km). We have begun assessing the performance and added-value of going to convection-resolving resolutions, within the HARMONIE configuration, concentrating on summer season precipitation over the Alps. We choose the Alps due both to the extreme topographic forcing of precipitation and because a well-documented, high-resolution observed precipitation data set is available for model evaluation. We have run HARMONIE, on the full Euro-CORDEX domain, for 6 summer seasons (May-September inclusive) spanning a range of representative summer precipitation outcomes over the Alps. HARMONIE is run at the two resolutions; 12.5km and 6.25km, with the output from the 12.5km model used in a double-nesting step to force an inner HARMONIE domain at 2.5km resolution centred on the Alpine region. This interior domain is run for the same 6 summer seasons twice, using either ALARO or AROME physics. Such an experiment protocol allows us to evaluate simulated precipitation statistics in the 3 HARMONIE versions; 12.5km, 6.25km and 2.5km (the latter forced by the 12.5km HARMONIE) over the common Alpine region. Furthermore, testing both ALARO and AROME in the 2.5km domain allows an assessment of the relative benefits of both schemes at high resolution, contrasting this with the importance of physics consistency across the lateral boundaries of the small Alpine domain, with ALARO physics used in the 12.5km driving model. This set of simulations is now close to completion and analysis begun, looking at precipitation variability across the range of model resolutions and physics packages. We envisage submission of an article on this subject early in 2014.

Based on these assessments, and the aforementioned technical developments in HARMONIE, we aim to start the 6.25km, 30-year EC-Earth-forced 30-year timeslice simulations during autumn/winter of 2013. Present and future climate timeslices can be run in parallel if disk space and core availability allows.

List of publications/reports from the project with complete references

As the project has only been running 6 months, no publications have yet arisen. The first publication, aimed for submission in September 2013, is attached to this report as a *work-in-progress* document.

Summary of plans for the continuation of the project
(10 lines max)

As outlined above, the latter half of 2013 will concentrate on 2 scientific articles detailing the performance of HARMONIE at a range of resolutions over Europe for the present climate forced by ERA-interim. Towards the end of 2013 and during 2014 the intended, high-resolution HARMONIE timeslices for Europe, forced by EC-Earth data, will be started. Depending on progress made with these timeslices we also aim to apply the same HARMONIE 6.25km configuration using both ERA-interim and EC-Earth boundary data to East Africa. Here we aim, in particular, to study potential changes in the precipitation variability, drought and flood risks, at 2°C global warming levels. Finally, SMHI is a partner in a new EU FP7 project, HELIX due to start in early 2014, which aims to assess climate impacts associated with even higher levels of global warming (e.g. 4°C and higher compared to pre-industrial conditions). The basic techniques developed in this project will be important for subsequent use in HELIX in the coming ~4-5 years, hence developments in this project form a key aspect of our forward looking dynamical downscaling activities.

Very high-resolution climate
runs over Europe; an evaluation

David Lindstedt, Petter Lind, Colin G. Jones, Erik Kjellström

Contents

1 Introduction

Accurate model projections of precipitation distribution, especially the frequency and intensity of wet (and dry) extremes, still remains one of the largest challenges in the climate model community. Current generation climate models, global and regional, struggle to accurately capture the observed intensity and frequency of precipitation distributions, deviating from observations most radically at the extreme high- and/or low-intensity tails of the distribution (e.g. Kjellström et al., 2010; Wehner, 2013), and thus lowering the confidence in the models for projecting changes in these features under climate change scenarios. One important reason for this discrepancy is likely the low resolution presently used in climate models, an issue which has been extensively discussed and studied (e.g. Wehner et al., 2010; Kendon et al., 2012; Hohenegger et al., 2008; Gent et al., 2010; Iorio et al., 2004). With the use of an atmosphere-only GCM run in an aqua-planet configuration, thus eliminating the influence of boundary conditions, Li et al. (2011) investigated the purely atmospheric precipitation-producing processes (i.e. model parametrizations and dynamics) and their dependence across resolutions. The results did not show any clear convergence when increasing resolution from $\sim 2.8^o$ to 0.35^o, however, precipitation extremes demonstrated larger sensitivity to resolution than mean climatology. This emphasizes the importance of high resolution when trying to simulate higher-order statistics of rainfall. Moreover, at mid-latitudes there is often a seasonal dependence on the added value from high resolution. Iorio et al. (2004) reported that an overall improvement at finer resolution in a set of GCM runs, on seasonal as well as daily basis, were mostly achieved in autumn and winter, as an increasingly larger portion of large-scale precipitation became explicitly resolved. For the other seasons, moist convective processes dominates and inadequacies in model physics leads to limited improvements in simulated rainfall.

Running GCMs at higher resolution than $\sim$50 km (a resolution often referred to as a threshold resolution for the ability to capture extreme precipitation events in models (e.g. Wehner et al., 2010)) is still generally too expensive, and therefore dynamical downscaling provides a mean to explore finer scale climate information and interactions, as they are able to capture the local and regional forcings. Several studies have been undertaken to study the horizontal resolution dependence in RCMs (Rauscher et al., 2010; Sharma and Huang, 2012; Larsen et al., 2013; Gao et al., 2006; Leung and Qian, 2003). The majority of these, as for GCM studies, reach the conclusion of an improved model response as the resolution increases, especially in regions of complex terrain. However, it is not always evident what is the primary cause of the direct improvement; the finer representation of local and regional forcings or the model physics. Gao et al. (2006) reported that sensitivity of the latter was more important than the former to accurately represent precipitation over complex terrain in East Asia. Furthermore, Larsen et al. (2013) included as well the sensitivity of simulated precipitation to the domain size, in addition to varied resolution. They concluded that, for the studied area, Denmark and surrounding areas, the larger domain results were superior those of the higher resolution.

Therefore, just increasing the resolution does not necessarily implies better results. Even though a finer mesh grid enables more processes to be resolved as well as stronger surface forcings, for example in association with topography and land ocean contrasts, the impact of these on the model response may be modified or even masked by artefacts and errors in the convection parametrization, in some cases even deteriorating the resulting

response (Pope and Stratton, 2002; Giorgi and Marinucci, 1996). For example, Wilcox and Donner (2007) could conclude that the difference in the simulated frequency of extreme rain events in using two different convection schemes (in otherwise identical model setup) was larger than the change in the frequency of heavy rain events associated with a 2-K warming using either scheme. Sharma and Huang (2012) investigated convergence in precipitation response using a range of resolutions in an RCM. They reported such a convergence at grid box size below ∼5 km, but also excessive amounts in comparison to observations for these scales and instead a better agreement compared to the standard 12 km run. They argued that the discrepancy may be connected to model physics being tuned to the standard resolution and parametrization schemes not being resolution independent. More importantly, as grid sizes start reaching below ∼10 km in RCM's, usually referred to as the "grey-zone" scale, the resolved vertical velocity becomes significant and a considerable part of the resolved condensation originates from convective updrafts. Thus, at these spatial scales, parametrizations eventually start to seriously violate underlying statistical assumptions upon which the schemes are based, hence, these have to become more sophisticated to account for the stronger interactions between local convection and meso-scale processes (e.g. meso-scale circulations) (Frank, 1983; Molinari and Dudek, 1992). Arakawa et al. (2011) advocates a unified cloud parametrization, enabling a smooth and continuous transition from coarse meshes to cloud resolving scales. Similarly, Gerard (2007); Gerard et al. (2009) have approached the "grey-zone" scale dilemma by developing a more unified parametrization than most other schemes, the "3MT" scheme. The characteristics of 3MT are:

- The use of condensation and transport terms directly instead of a parameterized detrainment coupled to a balanced subsidence (Piriou et al., 2007)

- Clean separation of resolved and sub-grid condensates avoids double counting.

- Prognostic closure instead of a diagnostic one relieves the need for a quasi-equilibrium hypothesis for which the validity at high resolution is questionable.

This makes the convective parameterization more physically sound and the need for higher resolution in climate modelling can be reached.

In this study we use the model system HARMONIE at ∼6 km resolution in which the 3MT scheme is applied in order to achieve an improved representation of higher order regional climate such as intense precipitation events. As HARMONIE has not been run before in climate mode for such an extended time period it is important to establish that the model accurately represents large scale climate. We further explore the model behaviour and examine if any added value can be seen by increasing the resolution from 15 to ∼5 km, particularly with respect to simulating precipitation intensity and frequency distributions.

2 Description of HARMONIE

HARMONIE (Hirlam Aladin Regional Mesoscale Operational NWP In Europe) is a seamless NWP model or framework where the components have been built through cooperation between several national meteorological services. The model system contains a suite of physical parameterization packages that are developed to be applicable to different resolutions: (i) ∼15 km ALADIN physics (Bénard et al., 2010), (ii) at resolutions traditionally

referred as the grey-zone (∼5 km), ALARO physics, and (iii) at convective resolving resolutions (∼2 km), AROME physics (Seity et al., 2011; Bubnová et al., 1995). The Rossby Centre targets regional climate simulations in the range ∼5-8 km horizontal resolution over the coming ∼5 years and hence has a focus on the performance of the ALARO physics package (Gerard et al., 2009; Gerard, 2007; Piriou et al., 2007).

2.1 Dynamics

HARMONIE is built based on the ALADIN non-hydrostatic (NH) and spectral dynamical core (Bénard et al., 2010; Bubnová et al., 1995; Váňa et al., 2008). It's based on a two-time level semi-implicit Semi-Lagrangian discretisation of the fully elastic equations in the atmosphere. In the vertical a mass-based hybrid pressure terrain-following coordinate is used (Simmons and Burridge, 1981; Laprise, 1992). For coarser resolutions there is an hydrostatic option of the dynamical core.

2.2 Surface

The surface parametrization framework in HARMONIE is SURFEX (Surface externalisée, (Masson et al., 2012)). It originates from the ISBA surface scheme (Noilhan and Planton, 1989) and has expanded to a larger concept. It is more of an external surface modelling system available off-line as well coupled to an atmospheric model. When coupled to an atmospheric model, SURFEX receives variables such as air temperature, humidity, wind and precipitation for every time step and then uses these values to compute average values for i.e momentum and surface energy fluxes. Information of the land surface properties in SURFEX is taken from the ECOCLIMAP database (Champeaux et al., 2005). Readers are referred do the SURFEX scientific documentation (Le Moigne, 2012) for a thorough description.

2.3 Radiation

The radiation parameterization in HARMONIE is a two-stream scheme with one band for solar and one for the thermal spectrum. It is developed to be flexible and fast, mainly to be used in NWP applications (Ritter and Geleyn, 1992). The cloud geometry assumes maximum overlap between adjacent cloud layers and clouds separated by clear air are independent. The treatment of cloud optical properties is updated according to Măsek (2005).

2.4 Moist processes

The convective parametrization scheme in HARMONIE is 3MT (Modular Multiscale Microphysics and Transport) (Gerard et al., 2009; Piriou et al., 2007; Gerard, 2007). 3MT is specifically developed towards a horizontal resolution of ∼ 5 km and treats the grey-zone challenge through a cascading approach. Instead of one scheme for deep convection (DC) and one for 'non-convective', i.e. resolved large-scale, clouds and the microphysics in these, where each scheme produces precipitation and there is a risk of double counting some processes, 3MT formerly separates the different processes and updates the prognostic variables in an internal state sequentially.

The first process to be handled is the representation of large-scale clouds where the calculation of cloud fraction follows Xu and Randall (1996). This scheme further computes

4

the resolved part of the condensation/evaporation. Condensates estimated at this step are saved until the corresponding condensates from the convective part has been computed and the sum is passed on to the microphysical package (Gerard et al., 2009). The microphysical processes are described similar to Lopez (2002) and handles five prognostic water phases, where the autoconversion, collection and evaporation are computed level by level. Details of evaporation, melting and treatment of sedimentation can be found in (Geleyn et al., 1994) and (Geleyn et al., 2008) respectively.

The turbulence parameterization is a pseudo-prognostic Turbulent Kinetic Energy (pTKE) scheme which is an extension of the Louis type vertical diffusion scheme (Louis, 1979), and a connection with the CBR scheme (Cuxart et al., 2000) is present mainly by the conversion of mixing lengths, adapted from Redelsperger et al. (2001). Further information of the direct implementation can be found in (Geleyn et al., 2006).

The deep convective updraft is a mass-flux scheme, where the closure is based on vertically integrated moisture convergence with prognostic variables instead of a steady-state cloud budget which many schemes written for coarser resolutions use (e.g. Tiedtke, 1989; Kain and Fritsch, 1993; Bechtold and Bazile, 2001). There is a clean separation in the output between condensation- and transport fluxes, where the DC condensation fluxes is added to the corresponding large-scale fluxes before entering the microphysics. The parameterization of the moist downdraft use the same prognostic variables as the DC updraft and the calculations are done in a corresponding way (Gerard, 2007).

3   Experiment design and evaluation data

3.1   Model setup

HARMONIE in climate mode (from here on HCLIM) was setup on a curvilinear grid with a conformal Lambert projection over Europe at two resolutions, 15 and 6.25 kilometres, HCLIM15 and HCLIM6 respectively. Integrations have been performed from 1998 to 2007 with four months of spinup time prior to this. The model is forced by ERA-Interim (ERA-I) at the lateral boundaries and by ERA-I SST every six hours, with linear interpolation in between. The domain size is $300x320$ grid boxes in horizontal for HCLIM15 and $720x800$ for HCLIM6. Both have 60 levels in vertical. The time step is 360 and 180 seconds respectively. In all figures the extension zone of eleven grid points have been removed.

3.2   Evaluation data

Table 1 lists the various data sets to be used for evaluating the results from the HCLIM runs. To the extent possible, we compare with gridded observational data sets, primarily the EOBS data set created for the ENSEMBLES project (Haylock et al., 2008). EOBS is based on station data of precipitation and temperature, and these were interpolated employing a three-step methodology; first monthly means were interpolated using thin-plate splines. Then daily anomalies were interpolated using kriging. The final step combines daily and monthly grids.
As observations of total cloudiness and surface energy fluxes are sparse and associated with large uncertainties for various reasons, we use both ground-based and satellite-based as well as model-based (reanalysis) data in the evaluation in order to cover as many aspects of uncertainties as possible inherent in each observation type (as discussed later on).

Observations of any climate variable are inevitably associated with constraints and limitations for a number of reasons, e.g. sampling frequency and coverage limitations, and deficiencies in measuring devices as well as calibration issues. This is particularly true for precipitation. As this study emphasize the evaluation of simulated precipitation, we would like to briefly discuss in more detail issues associated with precipitation observations.

The use of point measurements (station gauges), whether or not interpolated to a grid using more or less advanced interpolation methods, is standard in model evaluation, and is also employed here. However, systematic biases in gauge-based observations of precipitation can be substantial, especially in winter at high latitudes and in regions with complex terrain (Adam and Lettenmeier, 2003). The main factors contributing to the biases are wind turbulence induced undercatch, wetting losses, evaporation losses and underestimation of trace amounts (Yang et al., 2005), all conspiring to lower estimates compared to the real values. Furthermore, gauge measurements are, in principal, restricted to land areas and due to the fact that they can only sample events that occur over the gauges themselves the gauges generally undersample localized events, a prominent feature during the convectively active summer season. In complex terrain observations tend to be sparse and gauges are most often placed in valleys. This can lead to substantial underestimation of precipitation, especially extreme events during the winter season.

Due to these reasons, comparison of model grid-box averages with station-based observations (although sophistically interpolated to a grid) should thus be done carefully. Using high resolution observational data sets may improve on this deficiency. Therefore, in addition to EOBS, we include in this study a number of gridded national data sets (Table 1), that besides a higher spatial resolution are designed by applying optimal methods (in some cases including bias correction) and using underlying station data most appropriate to the specific region in question and thus should be closer to the truth compared to pan-European data sets.

4   Results

The majority of this section details the performance of HCLIM15 and HCLIM6 in simulating the large scale climate over Europe. This will be done by comparing the two runs, HCLIM6 and HCLIM15, to some standard evaluation data sets frequently used in the literature (including high-resolution observations where possible). Also, we contrast the HCLIM15 results to another, well established, model system; the Rossby Centre RCA4 atmospheric RCM, run at a similar horizontal resolution. When the general performance is established in a more or less standard setting, we further explore the model behaviour by examining the simulated climate in somewhat more detail, primarily for precipitation, inter-comparing HCLIM6 and HCLIM15 results and the impact of higher resolution on these.

4.1   Large-scale circulation

4.1.1   Seasonal means and variability

The geographical distribution of seasonal mean sea level pressure (SLP) for HCLIM and RCA4 and their differences to ERA-I is shown in figure 2. Overall, the large-scale circulation is very well represented in HCLIM, with biases being at most ± 2hPa in any

season (although larger biases sometimes occur in mountainous areas, primarily related to differences in topography and adjustment to sea level pressure). It is noteworthy that HCLIM simulates the interannual and seasonal variability (figs. 2, 3) with a higher accuracy than the established model RCA4. This gives confidence to HCLIM in reproducing the large-scale flow in a realistic manner.

In HCLIM, the main difference is positive (higher SLP) and seen most frequently over southern Europe, except for summer when a positive bias over Scandinavia is seen. To some degree analogous SLP bias patterns by season and region are also seen in RCA4. One reason for the positive bias seen over the Mediterranean region, with maximum downstream of the Alps, could in part be related to problems in the model to accurately simulate cyclonic development in connection with large topographic barriers (e.g Smith et al., 2006).

That HCLIM skilfully reproduces the large-scale circulation over Europe is also evident from the empirical PDFs of daily mean SLP. The distributions closely match those of ERA-I for both winter and summer, over land as well as over sea (fig. 3). We can note the positive bias seen in the Mediterranean region in the cold season as a small contraction of the distribution; there are more days (than ERA-I) with values in the mid-range and an indication of too few in the lower range. This may support the theory of possibly insufficient lee cyclogenesis in the model. In accordance with this, a small shift to higher values in the distribution is seen for south-east Europe as well.

4.2 Clouds, radiation and surface fluxes

Figure 4 presents seasonal means for cloud cover, comparing HCLIM to reanalysis (ERA-I), surface based observations (CRU), satellite product (CM-SAF) and to RCA4. There is a relatively large spread in the different data sets, reflected in the inconsistency of the model deviations. However, in spring and summer for Scandinavia and north-east (NE) Europe there is a consistent signal of too much clouds and thus seem to reflect a real deficiency in HCLIM6 with a 10-15% bias. In should be noted that in HCLIM cloud fraction is a two dimensional variable calculated in the radiation scheme where a cloud-overlap assumption has been made, Further, the large negative bias over the Atlantic is an artefact due to boundary conditions. The relaxation zone (8 grid points) gives spurious results near the inflow boundary, most salient for cloud cover.

The positive bias in cloud fraction over north and NE Europe seen in CM-SAF during winter should be interpreted carefully. Satellite products are highly uncertain at high latitudes during winter; when the ground is cold and maybe covered by snow underestimation of clouds is common (CM-SAF, 2005; Karlsson et al., 2007). The same pattern is seen when comparing to ISCCP (Rossow and Schiffer, 1991) (not shown) which is an established global satellite product. Consistent with this, the comparison with the CRU data set (based on ground measurements) do not exhibit this large bias during winter. Similarly, the positive bias over Iberian Peninsula could also be related to inaccuracies in satellite retrievals; over semi-arid regions satellites can overestimate cloudiness due to low emissivity on these surfaces, but also cases of overestimation have been found (CM-SAF, 2005).

Compared to RCA4, HCLIM6 has generally to much clouds in southern Europe and too little clouds in the northern part, curiously, the spatial extent of the positive bias in

spring/summer seem to match a similar pattern in RCA and HCLIM6 compared to both CM-SAF and CRU.

As the solar radiation budget at the surface is highly sensitive to cloud amounts, it is natural to follow the cloud fraction analysis with that of radiation. Instead of seasonal maps, we here investigate the annual cycles for Scandinavia and West-Europe (fig. 5). Compared to ERA-I, HCLIM underestimates short wave down-welling radiation (SWd) during spring and summer, and overestimates in winter consistent with the cloud cover bias. The annual cycle of long wave down-welling radiation (LWd) in HCLIM shows a consistent negative bias for all months and both regions, even during summer when there is an overestimation of cloud cover. However the largest deviation from ERA-I occurs during winter (10-15 Wm^{-2}) for both regions. The reason for a negative bias in LWd over West Europe and small positive bias in SWd, despite a fairly good agreement in cloud cover could be due to problems with the model clouds being too transparent because of too low liquid water content and/or wrong droplet size distribution. A more in depth study of the treatment of clouds in HCLIM is needed to investigate this.

Figure 11 shows the annual cycle of latent (LH) and sensible (SH) heat fluxes. Observations of these fluxes are generally poor, at least on the regional and continental scales, and therefore we compare to ERA-I. Soil moisture largely controls the partition of LH and SH through the incoming radiative energy but one should note that soil moisture values in ERA-I are constrained by assimilation of near surface humidity. Although the overall surface fluxes are in good agreement, there are some evident differences between the models and ERA-I, especially over continental Europe. In south-eastern Europe (and to some extent in western Europe), for instance, there is a rapid decrease in LH in early summer compensated by a subsequent increase in SH in HCLIM, which gives a simulated summer Bowen Ratio (BR=SH/LH) of ∼1-2 (not shown). This corresponds well with observations from an Italian site where the observed summer BR was in the range of 1.5-2 during a four year period (Jaeger et al., 2009) while ERA-I This is not seen in ERA-I (BR≈0.7), however it corresponds well with observations from an Italian site where the observed summer BR was in the range of 1.5-2 during a four years period (Jaeger et al., 2009). On the other hand the strong reversal in SH/LH ratios could be likely due to an excessive drying of soils in summer in these regions. As will be seen later, precipitation is lower compared to observations in summer in parts of southern Europe, and this is probably related to underestimation of cloud amount compared to CRU, CM-SAF and also seen in ISSCP (4), and correspondingly overestimation of SWd (not shown). These factors combine to accelerate a drying of the soils and later on during the season to an underestimation of evaporation that then feeds back on precipitation production causing it to be too low.

In Scandinavia, and east Europe, HCLIM overestimates both surface fluxes during winter which probably is caused by a warm bias in these regions (sec.4.3). During spring and summer, SH is lower compared to ERA-I for both HCLIM and RCA. In Scandinavia, there is a net shortage of radiative energy at the surface compared to ERA-I throughout the year, being most pronounced during summer. This shortage is due mostly to the underestimation of SWd radiation associated with an overestimation of cloud cover. In eastern Europe, on the other hand, the net radiative energy compares well with ERA-I (not shown), and the lower SH is compensated by an relatively high LH. The correlation between surface heat fluxes and precipitation is most relevant during convective condi-

8

tions. Thus, during spring/early summer, the larger latent heat flux in HCLIM (and RCA) could be related to strong precipitation simulated for eastern Europe (as will be shown later). The feedbacks involved with the hydrological cycle and energy budgets may in turn lead to significant effects on the surface temperature as well.

4.3   Two meter air temperature

4.3.1   Seasonal means

The simulated 2 metre temperature over Europe, as simulated by HCLIM, is approximately within $\pm 2\,^oC$ from EOBS (also if compared to ERA-I), with summer and autumn having the smallest biases (see fig. 6, 7). Furthermore, the biases are generally on the cold side in all seasons (however, not as cold as those in RCA4), being most pronounced in spring over southern and eastern Europe reaching 2-3 degrees lower than EOBS over extended areas. A large part of this could probably be related to an overestimation of precipitation in the same season (see below) causing a cooling effect from increased latent heat flux due to wetter soils (figure 11). A significant exception to the cold bias is the quite large warm bias in winter in northern Sweden, Finland and western Russia, where some areas reach a bias of up to 5-7 degrees. The temperature bias extends into spring but with a much weakened amplitude.

There are three technical aspects of the model setup going from NWP to climate mode that explain this bias: sea-ice fraction and deep soil temperature are constant during the simulation; lake surface temperature is taken from the bottom soil layer close to the lake (a good approximation in NWP application). This explains the very large positive temperature biases over the lakes. This is in fact the main reason to the warm bias due to the vast number of lakes in northern Europe.

In a coming version of HCLIM the surface parameterization will be improved by using a more physically based approach and a lake model. However, the influence of the warm bias in northern Europe during winter could explain the errors in both components of the surface fluxes (figure 11), but does not effect any other analysed parameters. Instead the result show a lack of clouds (compared to ERA-I) with a corresponding positive and negative bias in shortwave and longwave radiation respectively at the surface (figure 5). As said earlier, the biases in cloudiness are probably not only related to model errors but also to the accuracy of observations, especially in this region during the season with partly snow covered grounds. Also, snow cover is another controlling factor of temperature in this region in winter. An underestimation of snow cover may, e.g. through feedback mechanisms, cause or intensify a warm bias. Snow cover, though, has not been included in this analysis.

4.3.2   Annual cycle

The spatially averaged annual cycle for set of six European countries, figure 7, supports the analysis from the former section; the RCMs are too cold in most regions with a larger deviation in RCA4 than in HCLIM compared to ERA-I, being most emphasized in spring/early summer. However, as seen for France, when comparing to a more detailed observational data set (here SAFRAN with 8km resolution), the cold bias is reduced. The only positive biases in these regions occur in Sweden in winter (see earlier discussion) and in summer in Spain. Although the latter is relatively small ($\approx 0.5^oC$) it is prominent in

both HCLIM and RCA4. There is not much difference between the two HCLIM runs for any of the regions, however, where there is, HCLIM6 do end up closer to the reference data (e.g. in Germany, Switzerland, France and Spain).

4.4 Precipitation

4.4.1 Seasonal means

Figure 9 shows the geographical distribution of seasonal mean precipitation in HCLIM and RCA4 compared to gridded EOBS observations, see also Table 2 for statistical information. Because the seasonal means are produced from daily data from only ten years of data, a simple Student-T test is applied, and only statistically significant differences, at the 5% significance level, are shown in the maps.

The large-scale seasonal patterns of the deviations from EOBS are quite similar in the two RCMs. Overall, the models produce larger precipitation amounts compared to EOBS. In winter and summer the corresponding continental wide mean values are $\sim 20-30\%$ larger than observations in HCLIM (Table 2). The winter wet bias is most emphasized in eastern Europe, and drier conditions are mostly connected to complex terrain. For summer, a dipole pattern can be discerned; wetter in the north and negative or near-neutral in the south (except in connection to steep topography). The lower estimates are concentrated to south-eastern Europe. The 2m temperature revealed a warm bias compared to EOBS in summer suggesting too dry soils affecting the partitioning between sensible and latent heat fluxes in the energy budget so as to conspire to reduce precipitation, all components connected in a feedback process (see 4.2 and 4.3). In the transition seasons, one may note firstly that in autumn, differences are of generally smaller amplitudes and to a lesser extent statistically significant. Spring, however, stands out in the models as both HCLIM and RCA clearly produce excessive amounts over large parts of Europe (at least compared to EOBS), most significantly in eastern Europe, Scandinavia and over mountainous areas. Corresponding mean values are $\sim 60\%$ larger than EOBS in HCLIM (2.17, 2.07 and 1.32 mm/day in HCLIM15, HCLIM6 and EOBS respectively; the root mean square errors ($rmse$) are 0.80 and 0.76 mm/day in HCLIM15 and HCLIM6 respectively). Lastly, HCLIM has mostly smaller deviations than RCA for all seasons. For example, the large wet bias over eastern Europe in RCA in spring and summer is much reduced, although still quite large in and near the Baltic states.

Frequently, the largest differences are associated with areas of complex terrain, which is expected given that topography exerts such strong forcing on precipitation formation combined with the different degree of smoothness of topography in models and gridded observations as well as the sparseness of and uncertainties in observations in these areas (3.2). The bias signal is not consistent across different areas and seasons; for example in summer HCLIM produces more precipitation along the tops of mountain ranges and less in the surrounding slopes (e.g. in the Alps, Dinaric Alps, Pyrenees and the Carpathians), however, in winter there is a more mixed signal with overestimation on the windward side in for example southern Norway, British Isles and the Dinaric Alps but in the Alps there is a drier zone co-located at the tops or northern (windward) slopes. The reasons for these differences most probably depends on a number of factors, such as the representation of local and regional circulation patterns in HCLIM, and more detailed investigation is needed, though not undertaken here.

4.4.2 Annual cycle

The phase and amplitude of the annual cycles, figure 10 which in addition to EOBS include high-resolution observational data sets as well, are overall well captured by HCLIM. Differences exists, though, and both HCLIM and RCA seem to generally overestimate precipitation most of the time, most notably in winter and spring. Here, HCLIM show indications of a better resolved seasonal cycle than the RCA model. Again, regions with complex terrain stands out; over Switzerland, HCLIM do a reasonably good job capturing the seasonal evolution of the monthly precipitation. Conversely, RCA displays a dramatically different result where the annual cycle is almost reversed compared to HCLIM and observations. HCLIM has higher rainfall amounts during spring and summer compared to EOBS; however, by including the MetSwiss observations lends much more confidence in HCLIM as the comparison improves significantly. This indicates clearly the value of high-resolution reference data in complex terrain in these sort of evaluations.

There are also quite large spreads between models and observations in Norway. The MetNo high-resolution data have much higher amounts in winter than both the models and EOBS, although the former are in closer agreement than the latter. The very large difference between EOBS and MetNo again shows the issue of producing high-quality observational records in areas with steep topography, especially in the winter season when undercatchment introduce considerable biases. Although comparisons to standard observational products, like EOBS, prove useful when comparing general model behaviour, looking into more regional or local aspects require more detailed information. Figure 10 satisfactorily do show that by doing this reduce the model biases in most of the cases, even though all data have been aggregated on the coarsest grid, EOBS 25km.

In summary, on the seasonal and monthly basis, HCLIM (both at 6 km and 15 km resolutions) perform reasonably well compared to each other and observations. These results, together with the other basic variables discussed in previous sections, provide high confidence in the use of HCLIM in climate simulation mode. However, to get a more complete appreciation of the simulated precipitation, and also the benefit of running HCLIM at the higher resolution, one needs to consider the whole precipitation distribution and investigate the high time-resolution variability and tail-behaviour. This will be done in the following sections.

4.5 Variability and extremes

As for precipitation, the simulation of 2m temperature may be very dependent on horisontal resolution, particularly for regions with steep topography in the cold season. Therefore, we will start by briefly examining the empirical probability density functions (PDFs) of 2m temperature before moving onto precipitation which will be more focused on in the continuation of the study.

4.5.1 PDFs of two meter air temperature

Figure 8 shows the PDFs of 2m temperature for the winter and summer seasons. First of all, there is not any notable differences between HCLIM6 and HCLIM15, not even for areas with complex topography in either winter nor summer, which is a bit surprising. It could be that to really investigate the influence of resolved surface properties on the simulated tenperature one needs to spefiaclly extract these regions, otherwise the impact

may be swamped in the signal. Also, the smoothening of the data when aggregated onto a coarser grid could hide possible differences in the distributions.

Secondly, except for Sweden, the cold bias as seen in the time mean climate is evident as negative shifts in the temperature distributions. Otherwise, the widths and amplitudes of the distributions are rahter well simulated by HCLIM.

4.5.2 Precipitation; Annual distribution

Although it is key to be able to reproduce seasonal and monthly means of precipitation, a correct representation of the expected variability and spread, and most certainly of the frequency and intensity of extremes, is of even greater importance due to its impact on the surface hydrology.

4.5.3 Precipitation; Seasonal distributions

To further investigate the precipitation distributions, figures 12-13 presents empirical PDFs based on daily mean precipitation values for a number of sub-regions for winter and summer respectively. Where available, high-resolution observational data sets are included as well. Only wet days are included in the analysis, with a threshold set to 0.2mm. Here, all data have been aggregated to the EOBS grid, i.e. with a 25 km horisontal grid box spacing. Although this procedure reduce the amount of information that would otherwise be available at the native higher mesh grid resolutions, the figures anyway give a gross picture of the observed distributions and how well they are represented in HCLIM. Furthermore, the PDFs are calculated for intensities up to 100 mm/day, but it should be noted that for intensities above $\sim$50 mm/day (which is close to the $99.9^{t}h$ percentile in most sub-regions and seasons.

Evidently, HCLIM qualitatively reproduces the distributions in terms of both frequency and intensity and also the seasonal evolution. There are, though, interesting differences that also have a seasonal dependence. HCLIM clearly underestimates the frequency of moderate to strong events, from $\sim$10 up to $\sim$50 mm/day depending on season and region. The understimation is most prominent in summer and in central Europe (here represented by Germany and Switzerland). The bias becomes somewhat larger if you include days with 0-0.2 mm/day as they appear more often than in observations. The only clear exception to this, in these figures, is in Sweden during winter and spring when the model overestimate probabilities for moderately strong to strong intensitites.

As we have run HCLIM at a horisontal resolution of 6 km, within the so called "grey-zone" resolution range, it is important to evaluate the possible added value by using this finer grid compared to the more state-of-the-art 12-15 km. The differences in the PDFs between HCLIM6 and HCLIM15 are relatively small but notable. For low to moderate intensities they are almost indistinguishable, but for higher rates HCLIM6 tends to give higher probabilities (see for example Germany in winter and Sweden in spring). Additionally, far out in the tail, for very extreme values, there is more signal present from HCLIM6 than HCLIM15, i.e. it's more common (although with very low probability) with these very high rates in the former than in the latter.

Multiplying the raw histogram numbers by the mean precipitation rate in each bin yields the total precipitation amount contributed to the seasonal mean by each precipitation rate bin. Figures 14)-15) show these curves for winter and summer respectively, and they

clarify the differences between models and observations for the rainfall intensities that are most contributing. For instance, although the PDFs indicate that HCLIM underestimates rain rate probabilities for a large part of the distribution, HCLIM yields approximately the right amount (winter), or overestimates it (summer), for the low to moderate intensities ($\sim$1-10 mm/day). A more prominent overestimation in this rate range is seen in the spring season (not shown), a feature that is clearly reflected in the mean estimate discussed earlier (figure 9)). In general, the peak of the curves in figures 14) and 15), i.e. at the rate that contribute most to the total amount, agrees well between HCLIM and observations, in some cases in winter being closer to the high-resolution data than to EOBS. An exception is Switzerland during summer where the peak in the model is shifted to lower intensities ($\sim$4-6 and $\sim$8-10 mm/day respectively), however, as the peak is also higher in HCLIM it does not result in lower estimates of the seasonal mean.

In summary, these results indicates that not only the seasonal and monthly means are well reproduced in HCLIM, also the full distribution are overall in good agreement with obserfvations. However, the model have some identifiable problems with precipitation production for certain seasons and regions. The observed excess of precipitation in spring (and to a lesser extent in summer) is attributed to the too frequent low-to-moderate events in the model (which is the range that contributes most to the total amount). For moderate-to-strong precipitation events the model instead underestimate, except for the highest percentiles.

5 Conclusions and summary

5.1 Acknowledgements

References

Adam, J. C. and Lettenmeier, D. P. (2003). Adjustment of global gridded precipitation for systematic bias. *Journal of Geophysical Research*, 108(D9).

Arakawa, A., Jung, J.-H., and Wu, C.-M. (2011). Toward unification of the multiscale modeling of the atmosphere. *Atmospheric Chemistry and Physics*, 11(8):3731–3742.

Bechtold, P. and Bazile, E. (2001). A mass-flux convection scheme for regional and global models. *Q.J.R. Meteorol. Soc.*, 127:869–886.

Bénard, P., Vivoda, J., Mašek, J., Smolíková, P., Yessad, K., Smith, C., Brožková, R., and Geleyn, J.-F. (2010). Dynamical kernel of the Aladin-NH spectral limited-area model: Revised formulation and sensitivity experiments. *Quarterly Journal of the Royal Meteorological Society*, 136(646):155–169.

Bubnová, R., Hello, G., Bénard, P., and Geleyn, J. (1995). The arome-france convective-scale operational model. *Monthly Weather Review*, 123(2):515–535.

Champeaux, J. L., Masson, V., and Chauvin, F. (2005). ECOCLIMAP: a global database of land surface parameters at 1 km resolution. *Meteorological Applications*, 12(1):29–32.

CM-SAF (2005). Satellite Application Facility on Climate Monitoring: Products Validation Report Summary. Technical report. SAF/CM/DWD/PVRS/1.

Cuxart, J., Bougeault, P., and Redelsperger, J.-L. (2000). A turbulence scheme allowing for mesoscale and large eddy simulations. *Quarterly Journal of the . . .* , 126(Lilly 1967).

Dee, D., Uppala, S. M., Simmons, A. J., Berrisford, P., Poli, P., Kobayashi, S., Andrae, U., Balmaseda, M. A., Balsamo, G., Bauer, P., Bechtold, P., Beljaars, A. C. M., Van De Berg, L., Bidlot, J., Bormann, N., Delsol, C., Dragani, R., Fuentes, M., Geer, A. J., Haimberger, L., Healy, S. B., Hersbach, H., Hólm, E. V., Isaksen, L., Kållberg, P., Köhler, M., Matricardi, M., McNally, A. P., Monge-Sanz, B. M., Morcrette, J. J., Park, B. K., Peubey, C., De Rosnay, P., Tavolato, C., Thépaut, J. N., and Vitart, F. (2011). The ERA-Interim reanalysis: configuration and performance of the data assimilation system. *Quarterly Journal of the Royal Meteorological Society*, 137(656):553–597.

Frank, W. (1983). The cumulus parameterization problem. *Monthly Weather Review*, 111:1859–1871.

Gao, X., Xu, Y., Zhao, Z., Pal, J. S., and Giorgi, F. (2006). On the role of resolution and topography in the simulation of East Asia precipitation. *Theoretical and Applied Climatology*, 86:173–185.

Geleyn, J.-F., Balize, E., Bougeault, P., Deque, P., Ivanovici, V., Joly, A., Labbe, L., Piedelievre, J.-P., Piriou, J.-M., and Royer, J.-F. (1994). Atmospheric parametrization schemes in Meteo-France's ARPEGE NWP model. Article in Conference Proceedings. www.ecmwf.int.

Geleyn, J.-F., Catry, B., Bouteloup, Y., and Brožková, R. (2008). A statistical approach for sedimentation inside a microphysical precipitation scheme. *Tellus A*, 60(4):649–662.

Geleyn, J.-F., Váňa, F., Cedilnik, J., Tudor, M., Brožková, R., and Catry, B. (2006). ACDIFUS prog (or pseudo-TKE) and its ingredients. Report. http://www.rclace.eu/?page=74.

Gent, P. R., Yeager, S. G., Neale, R. B., Levis, S., and Bailey, D. A. (2010). Improvements in a half degree atmosphere/land version of the CCSM. *Climate Dynamics*, 34(6):819–833.

Gerard, L. (2007). An integrated package for subgrid convection , clouds and precipitation compatible with meso-gamma scales. *Quarterly Journal of the Royal Meteorological Society*, 730:711–730.

Gerard, L., Piriou, J.-M., Brožková, R., Geleyn, J.-F., and Banciu, D. (2009). Cloud and Precipitation Parameterization in a Meso-Gamma-Scale Operational Weather Prediction Model. *Monthly Weather Review*, 137(11):3960–3977.

Giorgi, F. and Marinucci, M. R. (1996). A Investigation of the Sensitivity of Simulated Precipitation to Model Resolution and Its Implications for Climate Studies. *Monthly Weather Review*, 124:148–166.

Harris, I., Jones, P., Osborn, T., and Lister, D. (2013). Updated high-resolution grids of monthly climatic observations – the CRU TS3.10 Dataset. *International Journal of Climatology*, page "to appear".

Haylock, M., Hofstra, N., Klein Tank, A., Klok, E., Jones, P., and New, M. (2008). A European daily high-resolution gridded dataset of surface temperature and precipitation. *Journal of Geophysical Research (Atmospheres)*, 113(D20119).

Herrera, S., Gutiérrez, J., Ancell, R., Pons, M., Frías, M., and Fernández, J. (2012). Development and Analysis of a 50 year high-resolution daily gridded precipitation dataset over Spain (Spain02). *International Journal of Climatology*, 32:74–85.

Hohenegger, C., Brockhaus, P., and Schär, C. (2008). Towards climate simulations at cloud-resolving scales. *Meteorologische Zeitschrift*, 17(4):383–394.

Iorio, J., Duffy, P., Govindasamy, B., Thompson, S., Khairoutdinov, M., and Randall, D. (2004). Effects of model resolution and subgrid-scale physics on the simulation of precipitation in the continental United States. *Climate Dynamics*, 23:243–258.

Jaeger, E. B., Stöckli, R., and Seneviratne, S. I. (2009). Analysis of planetary boundary layer fluxes and land-atmosphere coupling in the regional climate model CLM. *Journal of Geophysical Research*, 114(D17):D17106.

Johansson, B. (2002). *Estimation of areal precipitation for hydrological modelling in Sweden.* PhD thesis, Earth Sciences Centre, Dept Phys. Geog., Gothenburg University (Sweden).

Kain, J. and Fritsch, J. (1993). Convective parameterization for mesoscale models: The Kain-Fritsch scheme. *Meteorological Monograph., American Meteorological Society*, 46:165–170.

Karlsson, K.-G., Sedlar, J., Devasthale, A., Stengel, M., Lockhoff, M., Meirink, J. F., and Wolters, E. (2007). EUMETSAT SAF on CLIMATE MONITORING: Validation Report Cloud product GAC Edition 1. Technical report. SAF/CM/SMHI/VAL/GAC/CLD.

Kendon, E. J., Roberts, N. M., Senior, C. a., and Roberts, M. J. (2012). Realism of rainfall in a very high resolution regional climate model. *Journal of Climate*, 25(17):5791–5806.

Kjellström, E., Boberg, F., Castro, M., Christensen, J., Nikulin, G., and Sánchez, E. (2010). Daily and monthly temperature and precipitation statistics as performance indicators for regional climate models. *Climate Research*, 44:135–150.

Laprise, R. (1992). The Euler equations of motion with hydrostatic pressure as an independent variable. *Monthly Weather Review*.

Larsen, M. A. D., Thejll, P., Christensen, J. H., Refsgaard, J. C., and Jensen, K. H. (2013). On the role of domain size and resolution in the simulations with the HIRHAM region climate model. *Climate Dynamics*, 40(11-12):2903–2918.

Le Moigne, P. (2012). Surfex scientific documentation. Technical report.

Leung, L. R. and Qian, Y. (2003). The sensitivity of precipitation and snowpack simulations to model resolution via nesting in regions of complex terrain. *Journal of Hydrometeorology*, 4:1025–1043.

Li, F., Collins, W., Wehner, M., Williamson, D., Olson, J., and Algieri, C. (2011). Impact of horizontal resolution on simulation of precipitation extremes in an aqua-planet version of community atmospheric model (cam3). *Tellus A*, 63(5). http://www.tellusa.net/index.php/tellusa/article/view/15882.

Lopez, P. (2002). Implementation and validation of a new prognostic large scale cloud and precipitation scheme for climate and data assimilation purposes. *Quarterly Journal of the Royal Meteorological Society*, pages 229–257.

Louis, J. (1979). A parametric model of vertical eddy fluxes in the atmosphere. *Boundary-Layer Meteorology*, 7:187–202.

Masson, V., Le Moigne, P., Martin, E., Faroux, S., Alias, a., Alkama, R., Belamari, S., Barbu, a., Boone, a., Bouyssel, F., Brousseau, P., Brun, E., Calvet, J.-C., Carrer, D., Decharme, B., Delire, C., Donier, S., Essaouini, K., a. L. Gibelin, Giordani, H., Habets, F., Jidane, M., Kerdraon, G., Kourzeneva, E., Lafaysse, M., Lafont, S., Lebeaupin Brossier, C., Lemonsu, a., Mahfouf, J.-F., Marguinaud, P., Mokhtari, M., Morin, S., Pigeon, G., Salgado, R., Seity, Y., Taillefer, F., Tanguy, G., Tulet, P., Vincendon, B., Vionnet, V., and Voldoire, a. (2012). The SURFEXv7.2 land and ocean surface platform for coupled or offline simulation of Earth surface variables and fluxes. *Geoscientific Model Development Discussions*, 5(4):3771–3851.

MeteoSwiss (2010). Daily Precipitation (final analysis): RhiresD. http://www.meteoschweiz.admin.ch/web/de/services/datenportal/gitterdaten/precip/rhiresd.html. Federal Office of Meteorology and Climatology MeteoSwiss.

Molinari, J. and Dudek, M. (1992). Parameterization of convective precipitation in mesoscale numerical models-A critical review. *Monthly weather review*.

Mǎsek, J. (2005). New Paramerization of cloud optical properties proposed for model ALARO-0. Report. http://www.rclace.eu/?page=74.

Noilhan, J. and Planton, S. (1989). A simple parameterization of land surface processes for meteorological models. *Monthly Weather Review*.

Piriou, J.-M., Redelsperger, J.-L., Geleyn, J.-F., Lafore, J.-P., and Guichard, F. (2007). An Approach for Convective Parameterization with Memory: Separating Microphysics and Transport in Grid-Scale Equations. *Journal of the Atmospheric Sciences*, 64(11):4127–4139.

Pope, V. and Stratton, R. (2002). The processes governing horizontal resolution sensitivity in a climate model. *Climate Dynamics*, 19(3-4):211–236.

Quintana-Seguí, P., Moigne, P. L., Durand, Y., Martin, E., Habets, F., Baillon, M., Canellas, C., Franchisteguy, L., and Morel, S. (2008). Analysis of Near-Surface Atmospheric Variables: Validation of the SAFRAN Analysis over France. *Journal of Applied Meteorology and Climatology*, 47(1):92–107.

Rauscher, S. A., Coppola, E., Piani, C., and Giorgi, F. (2010). Resolution effects on regional climate model simulations of seasonal precipitation over Europe. *Climate Dynamics*, 35:685–711.

Rauthe, M., Heiko Steiner, Ulf Riediger, A. M., and Gratzki, A. (2013). A Central European precipitation climatology – Part I: Generation and validation of a high-resolution gridded daily data set (HYRAS). *Meteorologische Zeitschrift*, page "to appear". "accepted".

Redelsperger, J., Mahé, F., and Carlotti, P. (2001). A simple and general subgrid model suitable both for surface layer and free-stream turbulence. *Boundary-layer meteorology*, pages 375–408.

Ritter, B. and Geleyn, J. (1992). A comprehensive radiation scheme for numerical weather prediction models with potential applications in climate simulations. *Monthly Weather Review*.

Rossow, W. and Schiffer, R. (1991). ISCCP cloud data products. *Bulletin of the American . . .*, 72:2–20.

Schulz, J., Albert, P., Behr, H.-D., Caprion, D., Deneke, H., Dewitte, S., Dürr, B., Fuchs, P., Gratzki, A., Hechler, P., Hollmann, R., Johnston, S., Karlsson, K.-G., Manninen, T., Müller, R., Reuter, M., Riihelä, A., Roebeling, R., Selbach, N., Tetzlaff, A., Thomas, W., Werscheck, M., Wolters, E., and Zelenka, A. (2009). Operational climate monitoring from space: the EUMETSAT Satellite Application Facility on Climate Monitoring (CM-SAF). *Atmospheric Chemistry and Physics*, 9(5):1687–1709. http://www.atmos-chem-phys.net/9/1687/2009/.

Seity, Y., Brousseau, P., Malardel, S., Hello, G., Bénard, P., Bouttier, F., Lac, C., and Masson, V. (2011). The arome-france convective-scale operational model. *Monthly Weather Review*, 139(3):976–991.

Sharma, A. and Huang, H.-P. (2012). Regional Climate Simulation for Arizona: Impact of Resolution on Precipitation. *Advances in Meteorology*, 12.

Simmons, A. and Burridge, D. (1981). An energy and angular-momentum conserving vertical finite-difference scheme and hybrid vertical coordinates. *Monthly Weather Review*.

Smith, S. a., Doyle, J. D., Brown, a. R., and Webster, S. (2006). Sensitivity of resolved mountain drag to model resolution for MAP case-studies. *Quarterly Journal of the Royal Meteorological Society*, 132(618):1467–1487.

Tiedtke, M. (1989). A comprehensive mass flux scheme for cumulus parameterization in large-scale models. *Monthly Weather Review*.

Tveito, O. E., Bjørdal, I., Skjelvåg, A. O., and Aune, B. (2005). A GIS-based agro-ecological decision system based on gridded climatology. *Meteorological Applications*, 12(1):57–68.

Váňa, F., Bénard, P., Geleyn, J.-F., Simon, A., and Seity, Y. (2008). Semi-lagrangian advection scheme with controlled damping: An alternative to nonlinear horizontal diffusion in a numerical weather prediction model. *Quarterly Journal of the Royal Meteorological Society*, 134(631):523–537. http://dx.doi.org/10.1002/qj.220.

Vidal, J.-P., Martin, E., Franchistéguy, L., Baillon, M., and Soubeyroux, J.-M. (2010). A 50-year high-resolution atmospheric reanalysis over France with the Safran system. *International Journal of Climatology*, 30(11):1627–1644.

Wehner, M. F. (2013). Very extreme seasonal precipitation in the NARCCAP ensemble: model performance and projections. *Climate Dynamics*, 40(1-2):59–80.

Wehner, M. F., Smith, R. L., Bala, G., and Duffy, P. (2010). The effect of horizontal resolution on simulation of very extreme US precipitation events in a global atmosphere model. *Climate Dynamics*, 34(2-3):241–247.

Wilcox, E. and Donner, L. (2007). The frequency of extreme rain events in satellite rain-rate estimates and an atmospheric general circulation model. *Journal of Climate*, 20(1):53–69.

Xu, K. and Randall, D. (1996). A semiempirical cloudiness parameterization for use in climate models. *Journal of the atmospheric sciences*.

Yang, D., Kane, D., Zhongping, Z., Legates, D., and Goodison, B. (2005). Bias corrections of long-term (1973-2004) daily precipitation data over the northern regions. *Geophysical Research Letters*, 32.

Table 1: Evaluation data used in the study

Dataset	Description	Variables	Resolution	Reference
EOBS	Gridded obs. Version 7.0	T2m, Pr	0.25^o	Haylock et al. (2008)
CRU	Gridded obs. Version TS 2.1	clt	0.5^o	Harris et al. (2013)
ERA Interim	ECMWF Reanalysis	SLP, clt, SWd, LWd R_n, LH, SH	0.79^o	Dee et al. (2011)
PPS	CM-SAF Polar Platform System	clt, LWd	0.25^o	Schulz et al. (2009)
MSG	CM-SAF Meteosat Second Generation	SWd	0.25^o	Schulz et al. (2009)
MetNo	Gridded obs. Norway	Pr	1 km	Tveito et al. (2005)
PTHBV	Gridded obs.	T2m, Pr	4 km	Johansson (2002)
RhiresD	Gridded obs. Switzerland	Pr	2.2 km	MeteoSwiss (2010)
REGNIE	Gridded obs. Germany	Pr	1 km	Rauthe et al. (2013)
SAFRAN	Reanalysis France	T2m, Pr	8 km	Quintana-Seguí et al. (2008) Vidal et al. (2010)
Spain02	Gridded obs. Spain	T2m, Pr	0.2^o	Herrera et al. (2012)

Table 2: Statistics of seasonal precipitation for continental Europe. Units are mm/day for $mean$ and root mean square error ($rmse$). $nstd$ is the normalized standard deviation and R is the coefficient of correlation. Subscript S and T refers to spatial and temporal respectively. The uncertainty range is given by the 95% confidence interval from bootstrap computations using 1000 samples.

| | DJF | | | JJA | | |
	EOBS	HCLIM15	HCLIM6	EOBS	HCLIM15	HCLIM6
$mean$	1.54 ± 0.01	2.04 ± 0.02	1.89 ± 0.02	1.57 ± 0.02	2.07 ± 0.02	1.92 ± 0.02
$nstd_S$	0.64 ± 0.01	0.62 ± 0.01	0.72 ± 0.02	0.69 ± 0.01	0.64 ± 0.01	0.71 ± 0.01
$rmse_S$		0.65 ± 0.03	0.59 ± 0.03		0.50 ± 0.02	0.46 ± 0.02
R_S		0.66	0.69		0.91	0.90
$nstd_T$	0.34 ± 0.01	0.29 ± 0.01	0.31 ± 0.01	0.31 ± 0.02	0.26 ± 0.01	0.28 ± 0.01
$rmse_T$		0.49 ± 0.04	0.40 ± 0.03		0.52 ± 0.03	0.46 ± 0.03
R_T		0.84	0.81		0.67	0.64
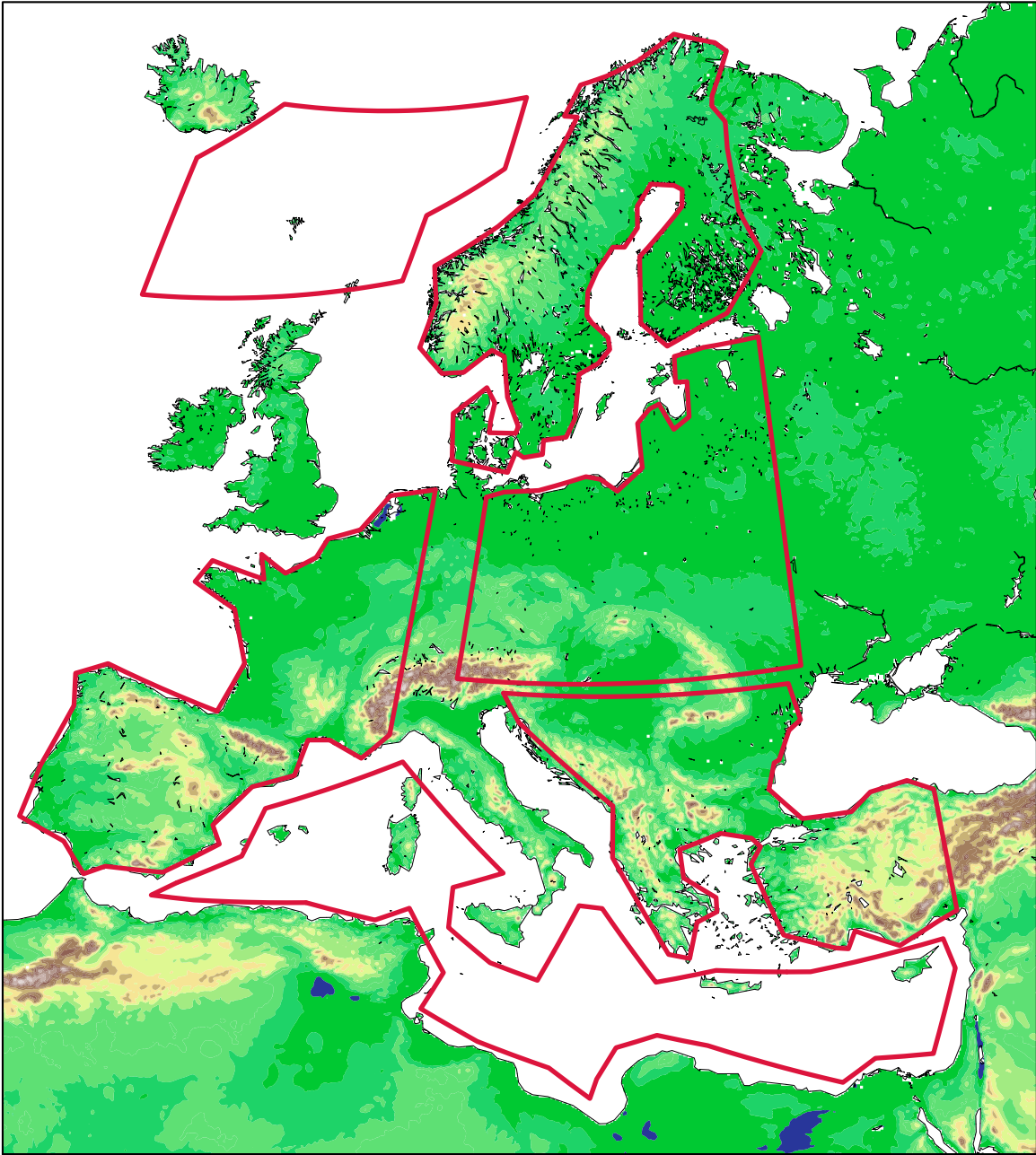
Figure 1: Topography and European sub-areas used in analysis; Scandinavia, West Europe, East Europe, South-East Europe, North Atlantic and Mediterranean.
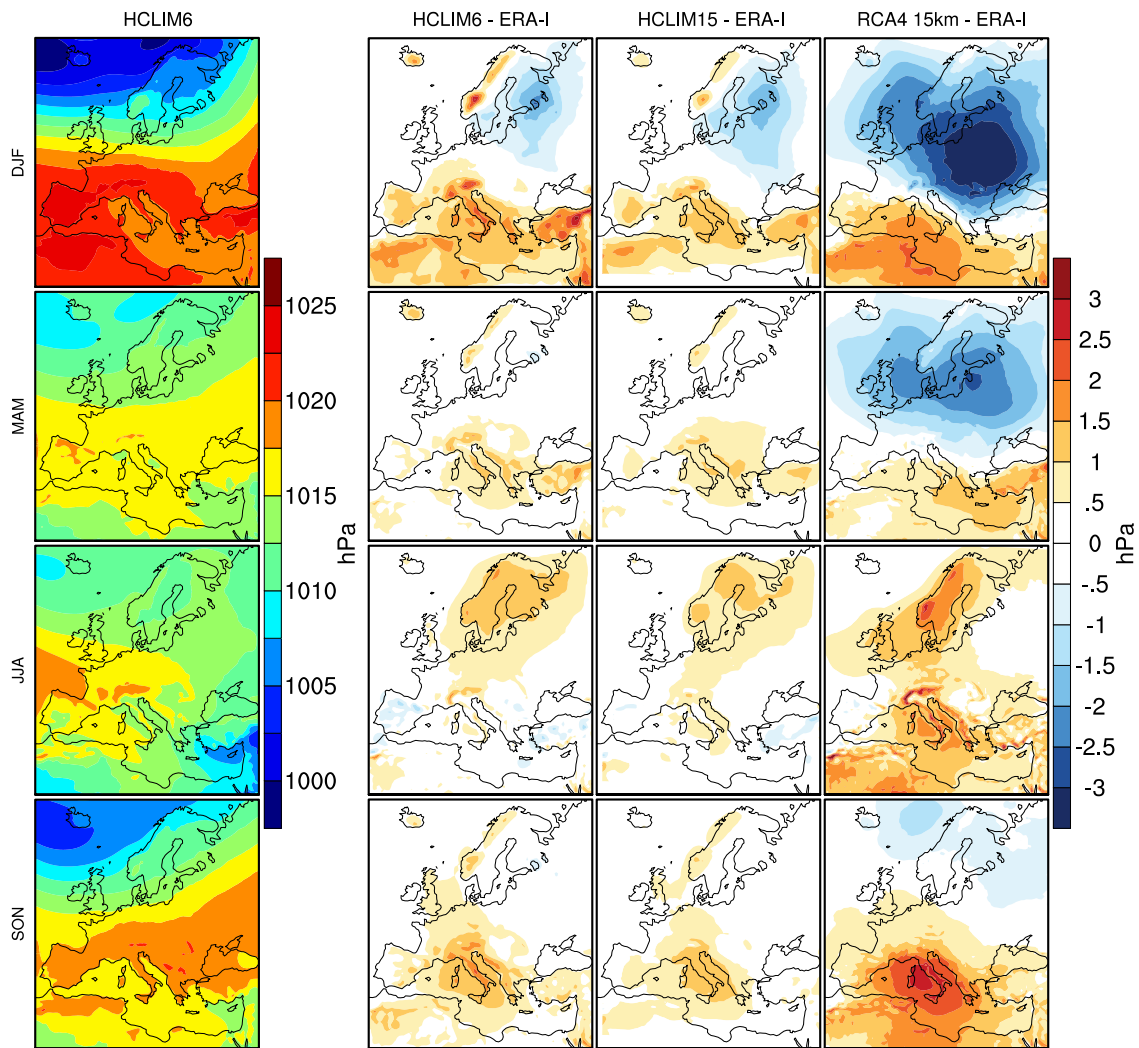
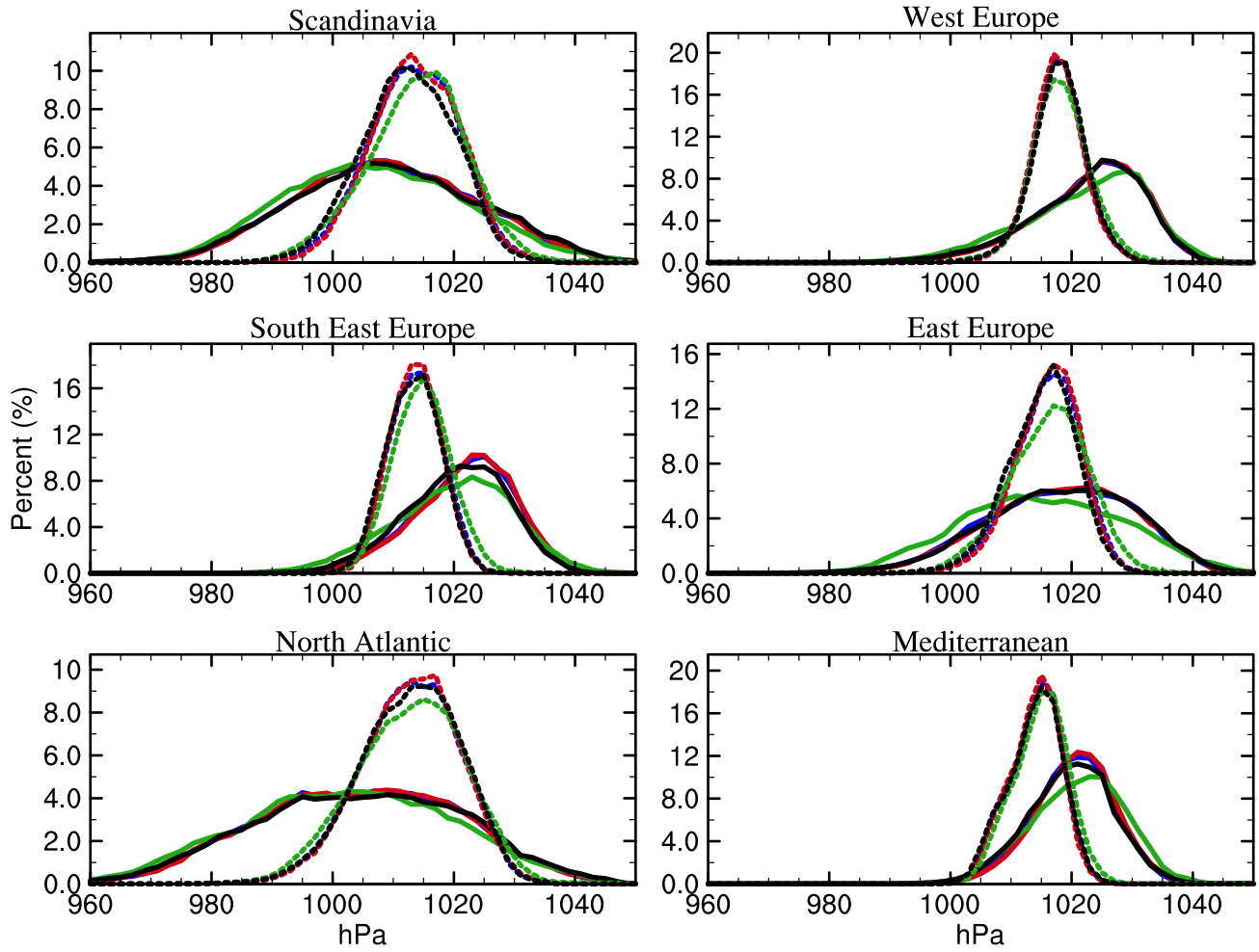Figure 2: Seasonal mean for mean sea level pressure

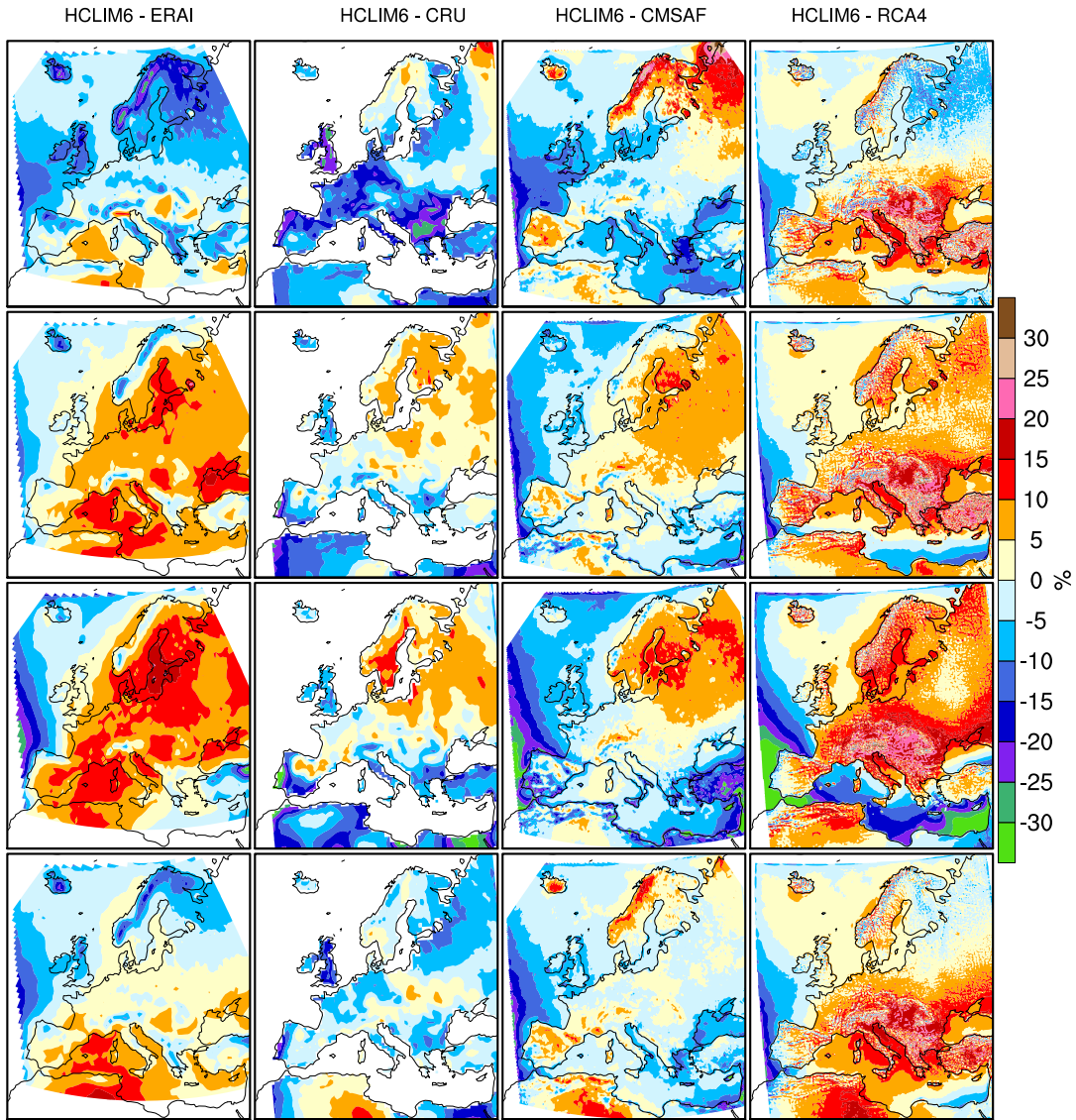Figure 3: Winter (solid lines) and summer (dotted) pdf's for sea level pressure

Figure 4: Seasonal mean for total cloud cover with reference to ERA-I, CRU and CMSAF PPS.
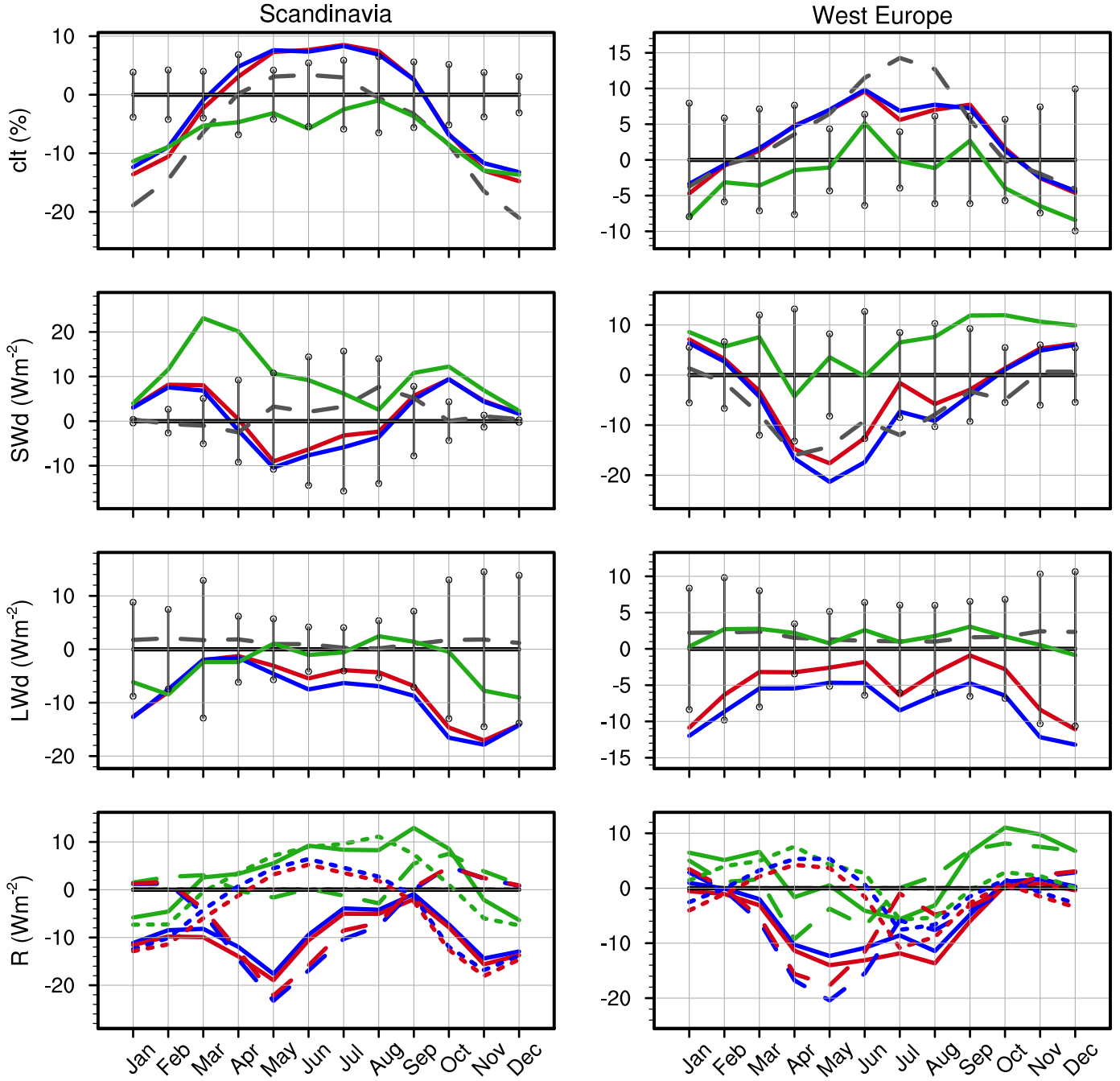
Figure 5: Annual cycle bias for cloud fraction (clt), down-welling thermal radiation (LWd), down-welling solar radiation (SWd) and surface net radiation budget (R_n).
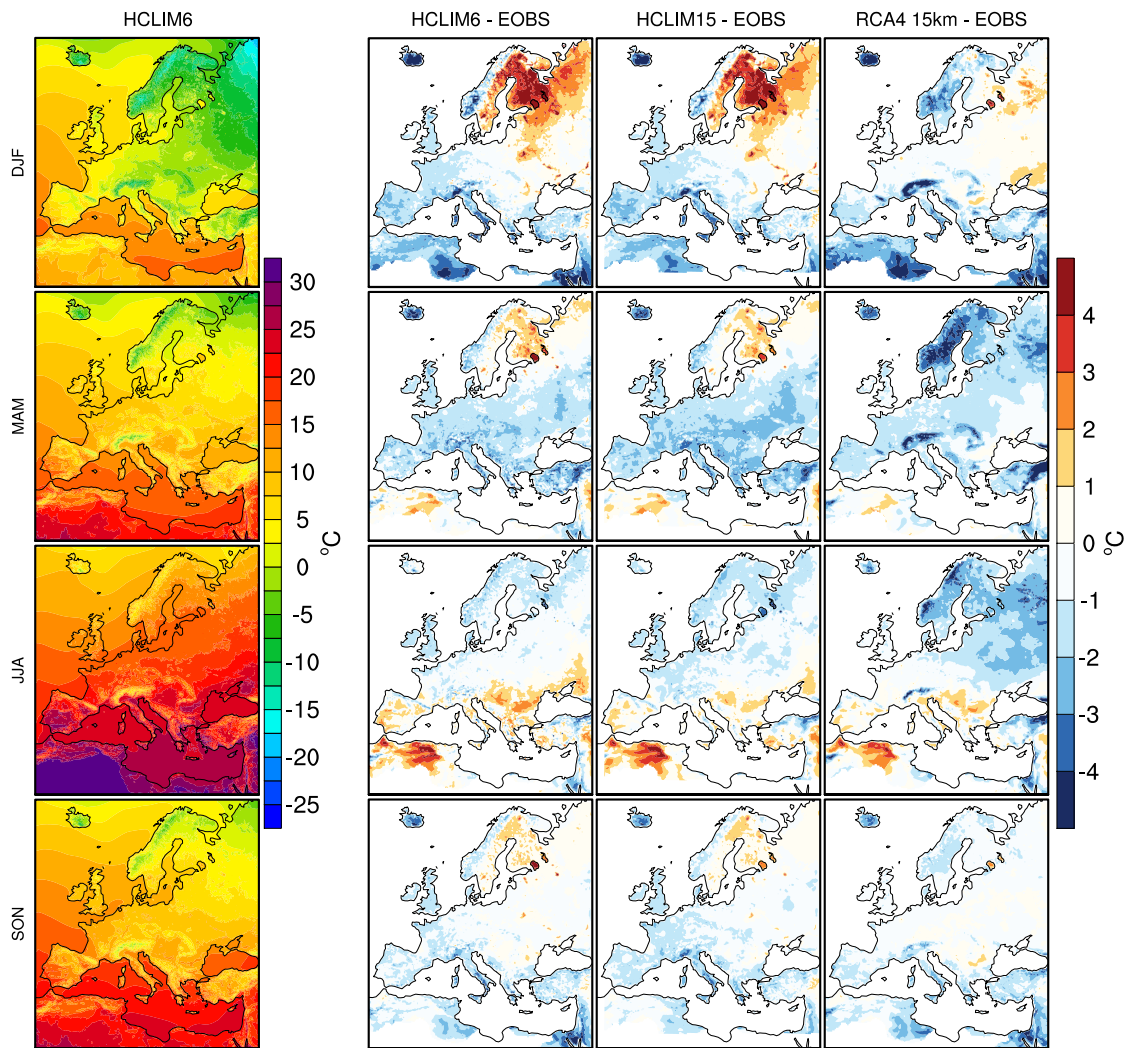
Figure 6: Seasonal mean for 2 meter temperature
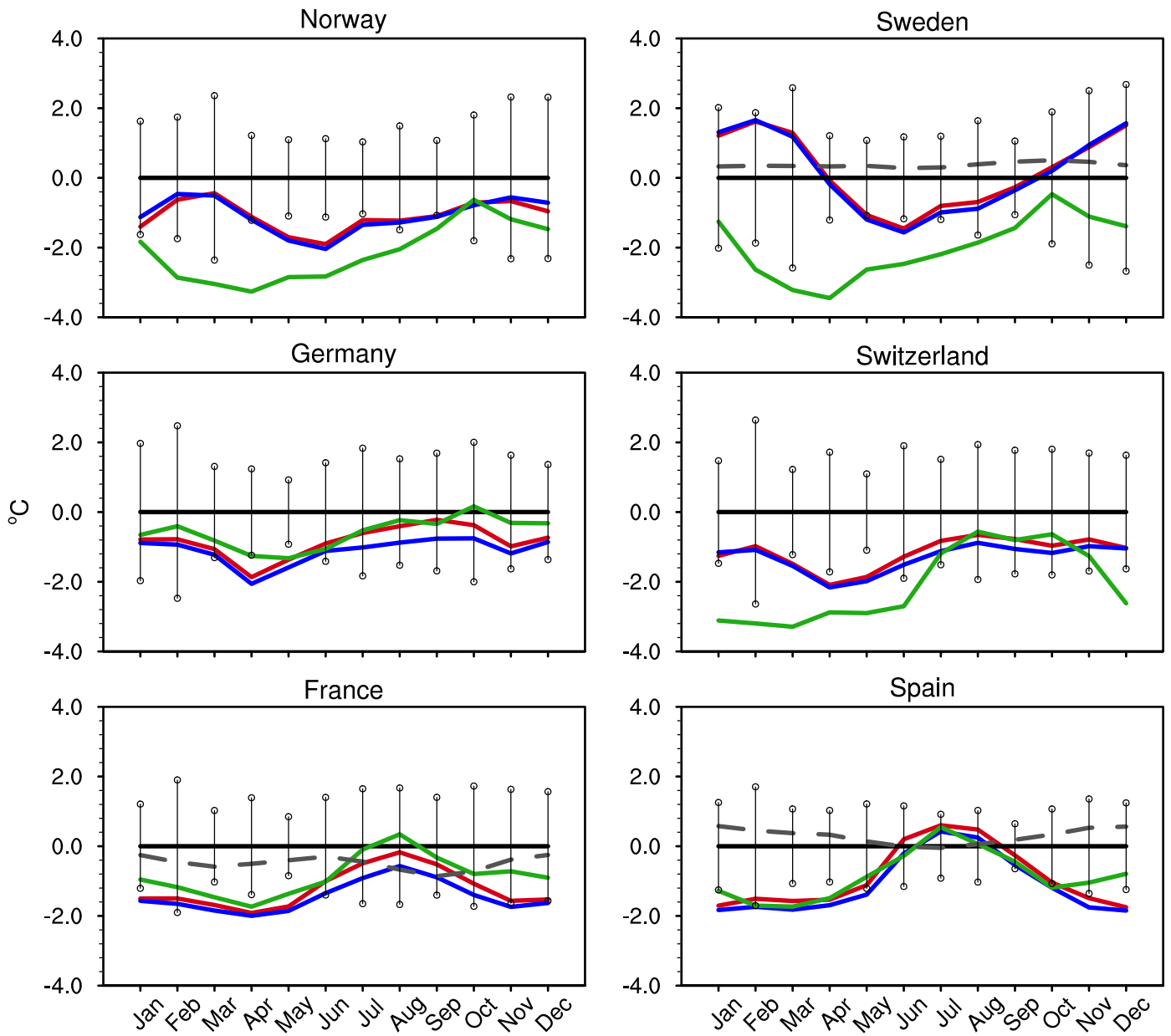
Figure 7: Annual cycle for 2 meter temperature
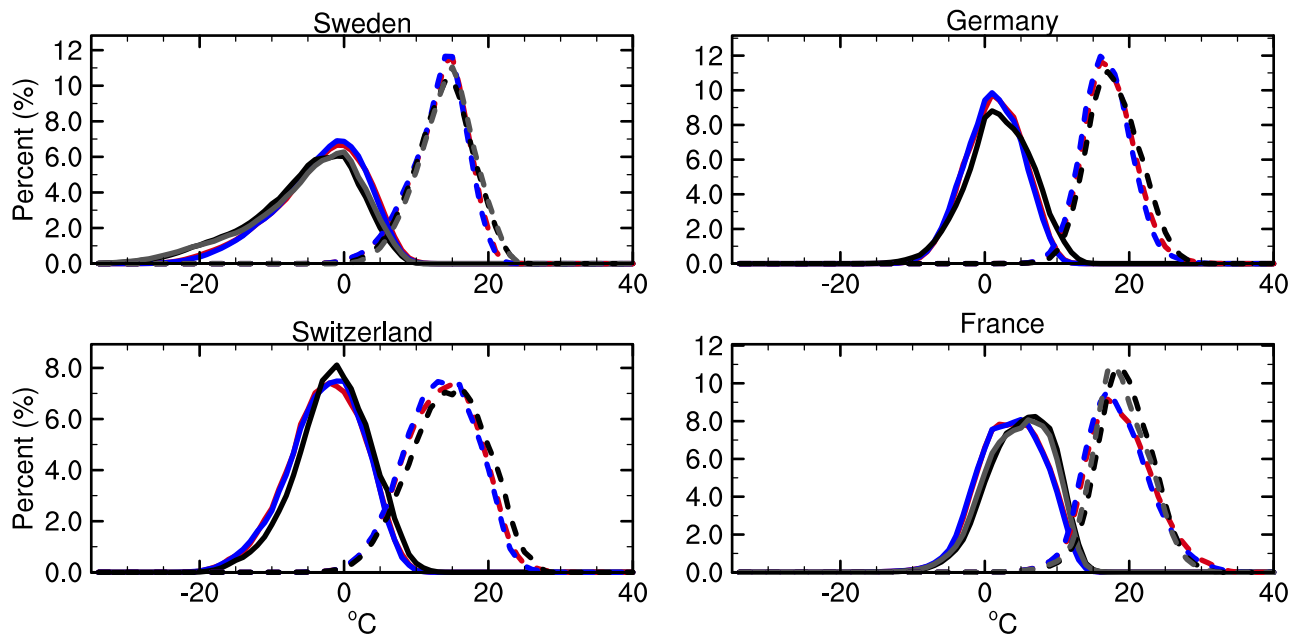
Figure 8: PDF for winter (DJF, solid lines) and summer (JJA, dashed lines) 2 meter temperature.
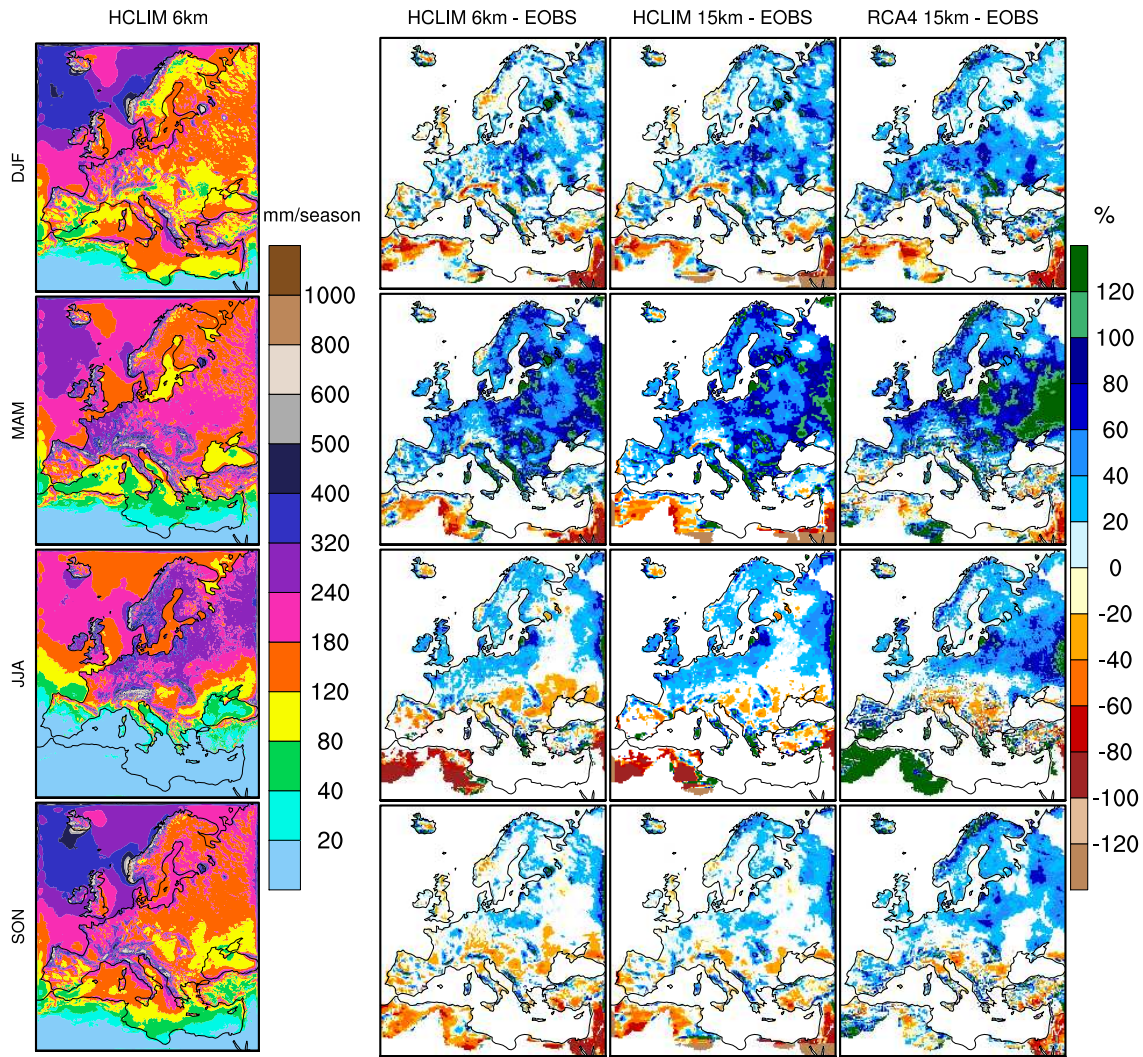
Figure 9: Seasonal mean for total precipitation. White areas (over land) indicate not statistically significant differences at the 5% level between model and observations and these grid points have been excluded.
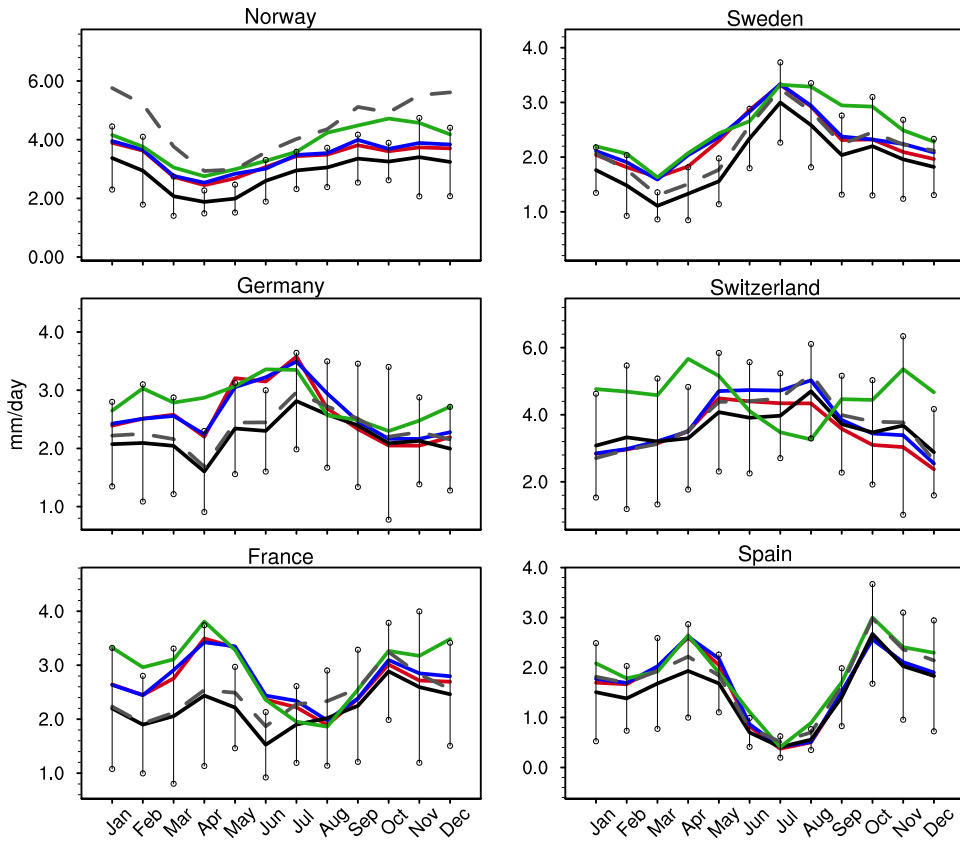
Figure 10: Annual cycle for precipitation
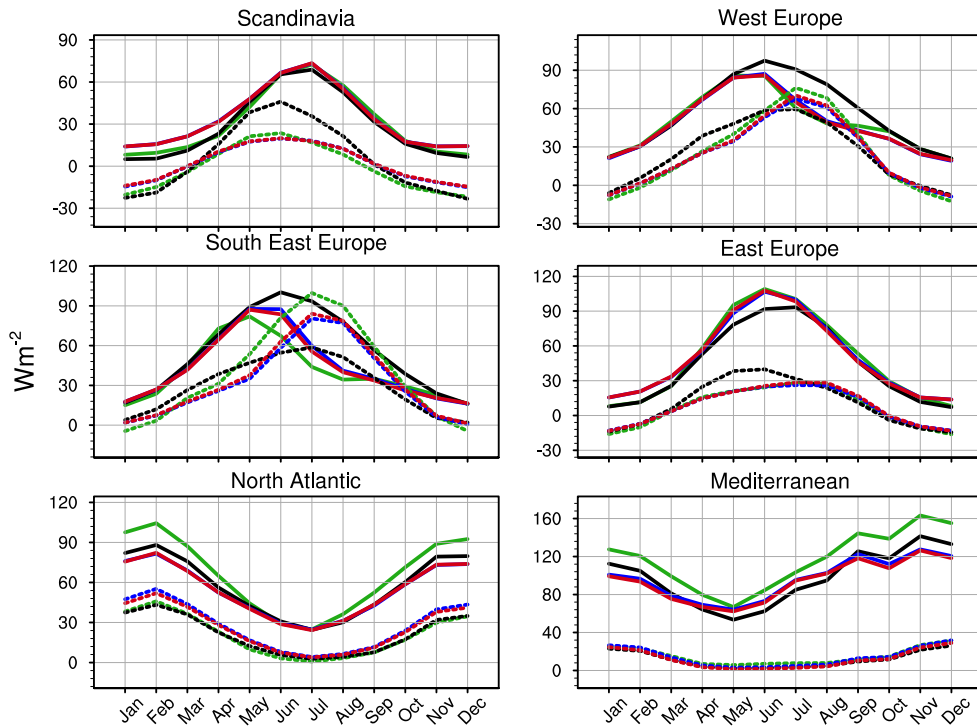
Figure 11: Latent (solid) and sensible (dotted) surface heat fluxes for ALARO, RCA and ERA Interim.

29
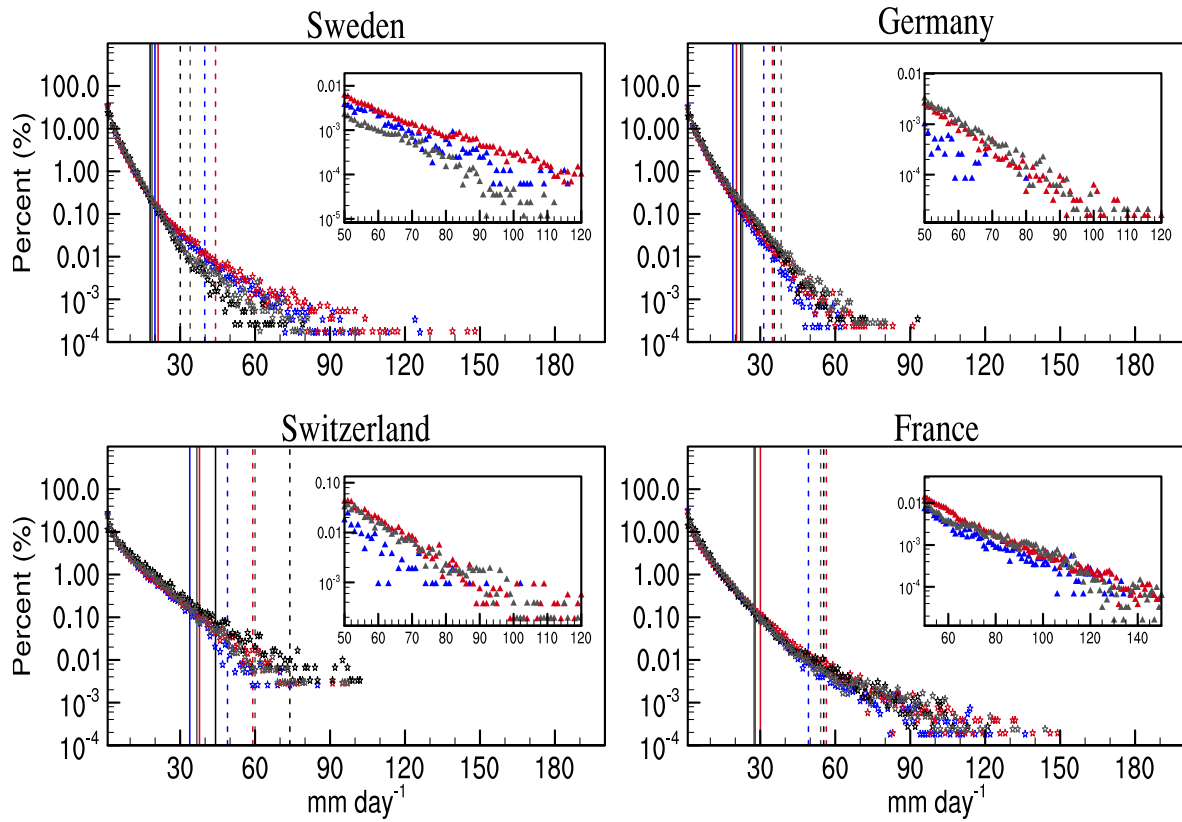
Figure 12: The PDF for DJF daily mean precipitation
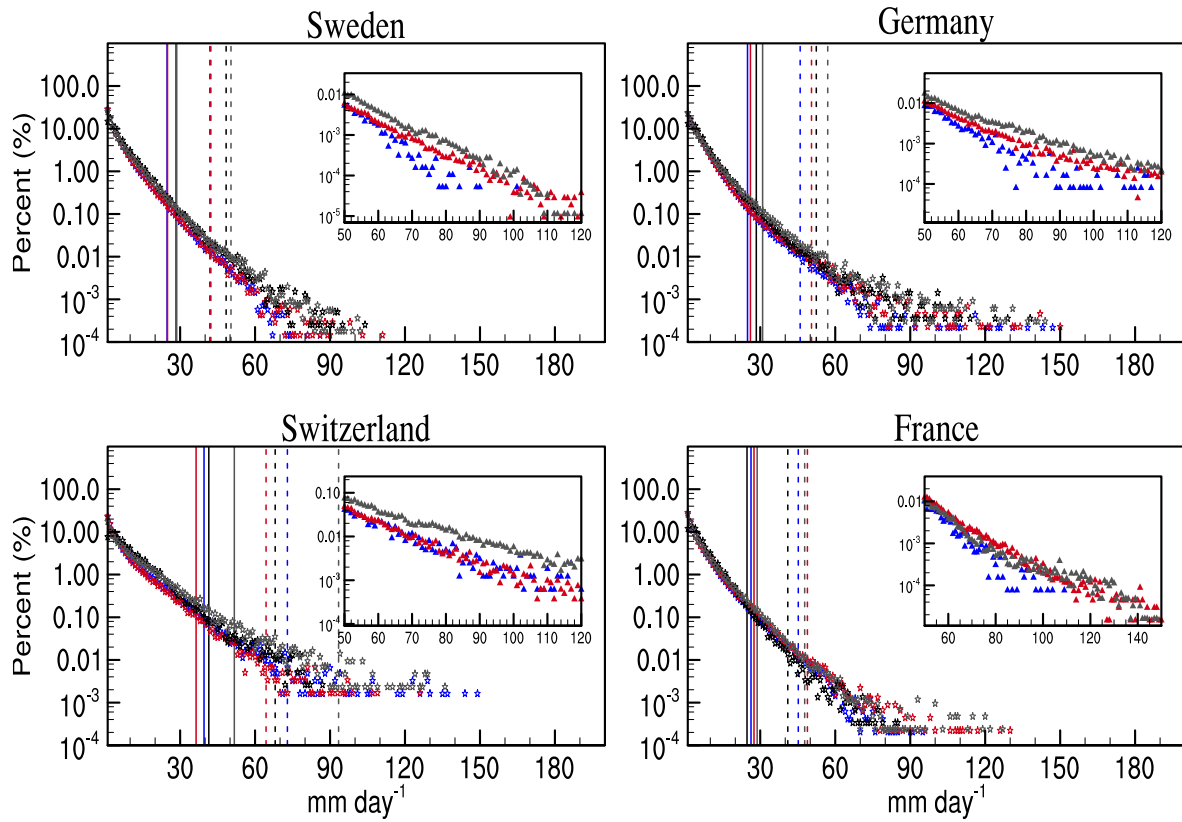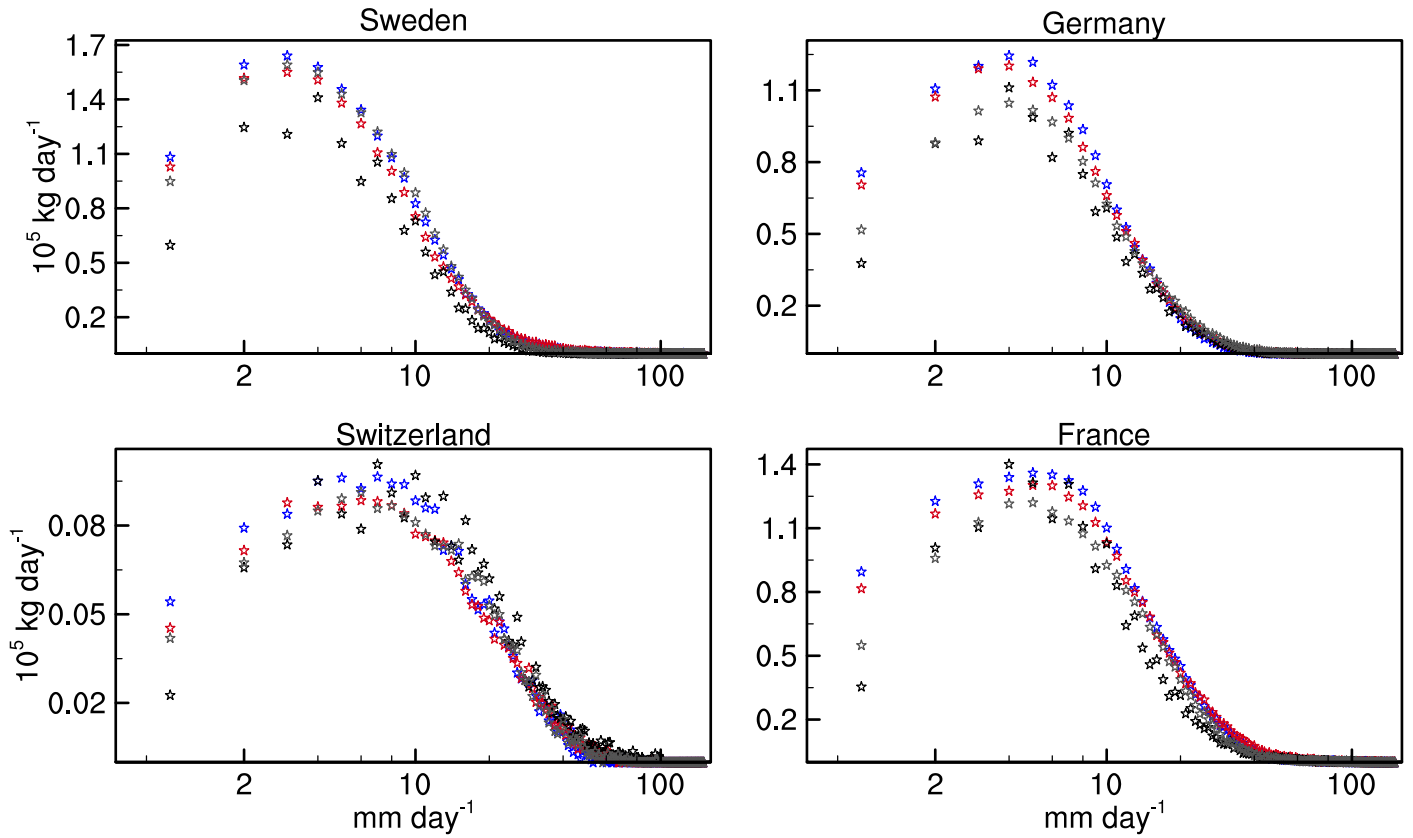
Figure 13: The PDF for JJA daily mean precipitation

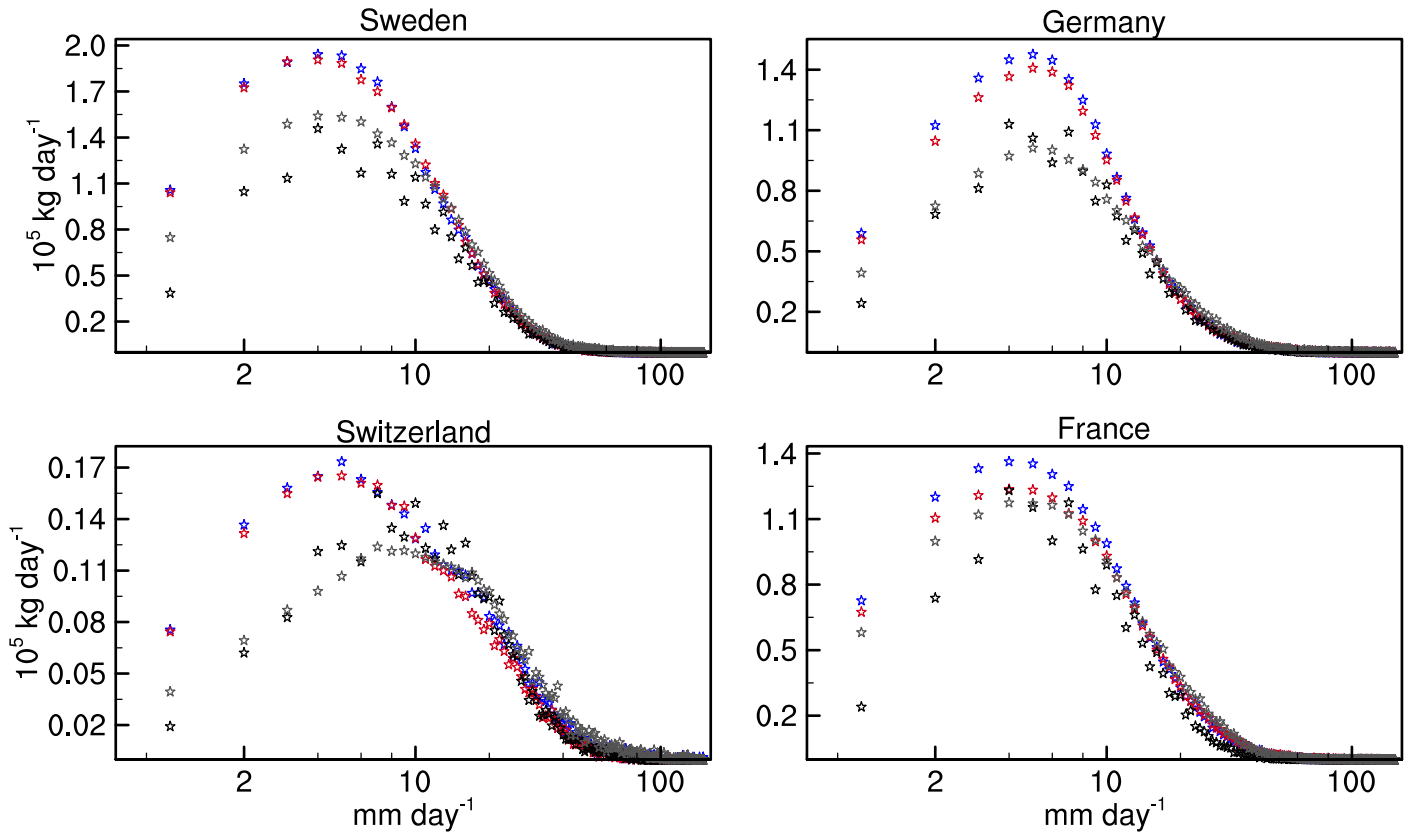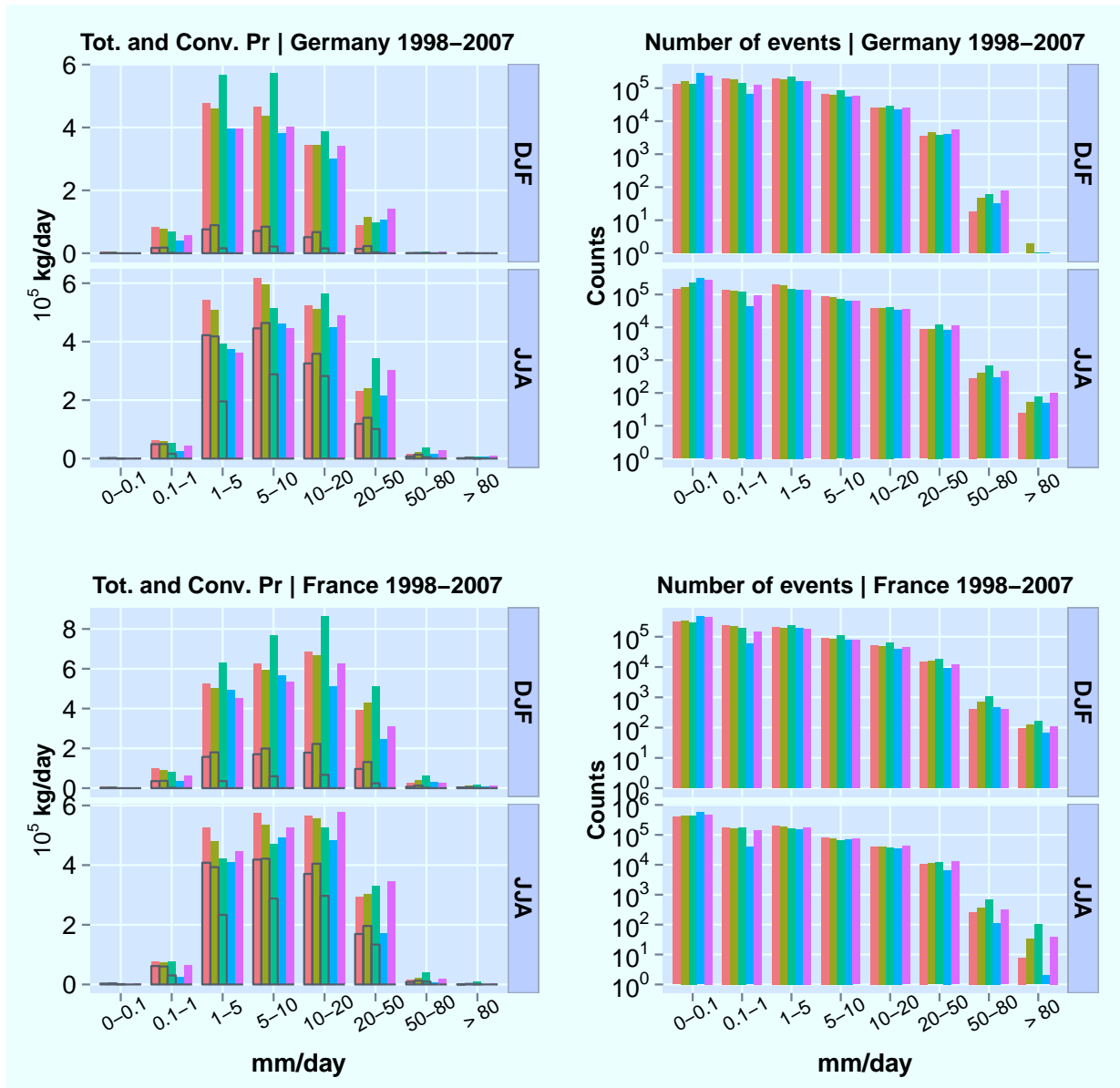Figure 14: Winter precipitation amount by rate.

Figure 15: Summer precipitation amount by rate.

Figure 16: Barplot of precipitation ...